PASSIVE

SHOCK

ISOLATION

**BARRY CONTROLS
ENGINEERING DEPARTMENT**

BARRY CONTROLS

Passive Shock Isolation   Part I

Passive shock isolation is discussed in terms of the performance of unidirectional single-mass isolation systems subjected to idealized forms of shock excitation. The nature of shock environments and the fundamental principles of passive shock isolation are presented. Selection of an isolator design involves achieving an acceptable combination of maximum acceleration (or force) and displacement response magnitudes. Analytical design data are provided for this purpose, including the effects of shock pulse shape and time duration, isolator damping, and isolator nonlinear stiffness characteristics. Optimum design parameters are established where applicable.

Shock excitation of a mechanical system causes the position of the system to change radically in a relatively short period of time. It may be defined in terms of a sudden variation of force applied to the system, or by displacement, velocity, or acceleration shock pulses imposed upon a particular point or points in the system. Mitigation of the effect of shock excitation may be achieved by inserting an isolator having appropriate stiffness and damping characteristics between the system being protected and the source of shock excitation.

Engineering solutions of shock isolation problems involve four basic tasks:

- ☐ Definition of shock excitation characteristics
- ☐ Specification of isolation system performance characteristics
- ☐ Analytical design of shock isolators
- ☐ Hardware mechanization of analytical design

The first task is concerned with analyzing the dynamic environment to arrive at a definition of shock excitation characteristics. This involves mathematical modeling of the shock environment and was discussed by the author in a previously published *Sound and Vibration* article.[1] The second task involves determining the required performance characteristics of the shock isolation system which is usually expressed in terms of an acceptable combination of maximum acceleration (or force) and displacement response magnitudes. The isolation system performance specification is generally based on such considerations as equipment fragility, structural integrity, clearance availability and shock isolator strength requirements. Analytical design of the shock isolator to theoretically provide the required performance characteristics for the particular shock environment is the third task involved. Finally, the analytical design of the shock isolator must be reduced to a hardware design; this task involves hardware mechanization wherein various isolator mechanisms are examined to determine the best one for the particular application being pursued. The

Nomenclature

Symbols and definitions of parameters used in this article are presented below. Shown in parentheses are the units of the parameters in terms of force (F), length (L), and time (T). The conventional dot-notation is used to indicate differentiation with respect to time; e.g., $\ddot{a}(t) = d^2a/dt^2$. A combination of dot-notation and a zero subscript is used to indicate the peak magnitude of a time-derivative parameter; e.g., $\ddot{a}_0$ represents the peak magnitude of $\ddot{a}(t)$.

Isolation System Parameters

m	= rigid mass of isolated body (FT^2/L)
k	= linear stiffness coefficient (F/L)
k_0	= initial linear stiffness (F/L)
k_1	= final linear stiffness (F/L)
N	= ratio of damper coupling stiffness to load-carrying stiffness, dimensionless
C	= viscous damping coefficient (FT/L)
C_c	= $2(km)^{1/2}$ = critical viscous damping coefficient (FT/L)
ζ	= C/C_c = viscous damping ratio, dimensionless
ω_0	= $(k/m)^{1/2}$ = undamped natural angular frequency $(1/T)$
f_0	= $\omega_0/2\pi$ = undamped natural frequency $(1/T)$
τ_0	= $1/f_0$ = undamped natural period (T)
δ_{st}	= static deflection (L)
$F(\delta)$	= undamped isolator force (F)
n	= exponent value, dimensionless
ϵ_n	= nonlinear stiffness coefficient (F/L^n)
ϵ_2	= quadratic stiffness coefficient (F/L^2)
ϵ_3	= cubic stiffness coefficient (F/L^3)

Excitation Parameters

$a(t)$	= displacement of foundation (L)
A_0	= $\ddot{a}_0/g$ = peak magnitude of foundation acceleration, dimensionless $(g's)$
A_s	= $\ddot{a}_s/g$ = sustained magnitude of foundation acceleration, dimensionless $(g's)$

$P(t)$ $\quad$ = force applied to isolated mass (F)

P_0 $\quad$ = peak magnitude of force excitation (F)

P_s $\quad$ = sustained magnitude of force excitation (F)

Δ_{st} $\quad$ = equivalent static deflection (L)

I $\quad$ = impulse (FT)

V_1 $\quad$ = initial velocity (L/T)

V_2 $\quad$ = final velocity (L/T)

V $\quad$ = velocity change (L/T)

h $\quad$ = free-fall height (L)

t_0 $\quad$ = shock pulse time duration (T)

t_r $\quad$ = rise time of shock excitation (T)

t_e $\quad$ = shock pulse effective time duration (T)

Response Parameters

$x(t)$ $\quad$ = absolute displacement of isolated mass (L)

X_{max} $\quad$ = maximum displacement magnitude of isolated mass (L)

$A(t)$ $\quad$ = $\ddot{x}(t)/g$ = acceleration of isolated mass, dimensionless $(g's)$

A_{max} $\quad$ = $[\ddot{x}(t)]_{max}/g$ = maximum acceleration magnitude of isolated mass, dimensionless $(g's)$

$\delta(t)$ $\quad$ = $x(t) - a(t)$ = relative displacement across isolator (L)

δ_{max} $\quad$ = maximum relative displacement across isolator (L)

$F_T(t)$ $\quad$ = force transmitted to foundation (F)

$(F_T)_{max}$ = maximum magnitude of force transmitted to foundation (F)

$T_s(\omega_0 t)$ = shock transfer response function, dimensionless

$H_s(\omega_0 t)$ = shock amplification response function, dimensionless

T_s $\quad$ = shock transmissibility, dimensionless

H_s $\quad$ = shock amplification factor, dimensionless

General

t $\quad$ = time (T)

ω $\quad$ = angular frequency $(1/T)$

f $\quad$ = $\omega/2\pi$ = frequency $(1/T)$

g $\quad$ = acceleration of gravity (L/T^2)

Subscripts

o $\quad$ = peak magnitude, maximum allowable value, or zero damping
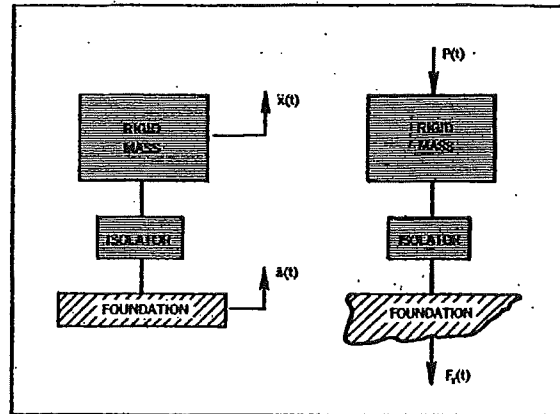
op $\quad$ = optimum value

Figure 1 — Schematic diagrams of idealized shock isolation systems for (a) shock excitation of the foundation and (b) shock excitation of isolated mass.

present article is concerned primarily with the analytical design of shock isolation systems.

Shock and vibration isolation systems can be generally categorized as being *linear* or *nonlinear*, depending on whether or not their dynamic response is described by linear differential equations with constant coefficients. They can be further categorized as *active* or as *passive*, depending on whether or not external power is required for the isolator to perform its function.[2] Active isolation systems are beyond the scope of this article and, therefore, only passive isolation systems are considered.

The essential features of a passive isolator are a resilient load-supporting mechanism (stiffness) and an energy dissipating mechanism (damping). Typical passive isolators employ metallic springs, elastomers, wire mesh, wire cable, pneumatic springs, elastomeric foams, and combinations of these or other cushioning devices.

Large-scale digital and analog computers have found wide use in the solution of complex shock isolation problems, where the effects of multi-degree-of-freedom motions and isolator nonlinearities can be accommodated. However, in the absence of the availability of such computers or the time to engage in full-scale computer simulation of the problem, much can be learned from a simplified mathematical model of the shock isolation problem. Furthermore, a fundamental understanding of shock isolation is more readily achieved by consideration of simplified versions of the problem. With this understanding, engineers with limited expertise can improve their communication with dynamics specialists on complex problems, and can learn to successfully apply commercially available products for problems of a less complex nature.

For the purpose of this article, the following simplifying assumptions are made. The isolation system is considered to be comprised of a rigid mass supported on a rigid foundation by a single isolator undergoing unidirectional dynamic motion. Sche-

matic diagrams of idealized shock isolation systems are illustrated in Figure 1 where: (a) the shock excitation is represented by an acceleration $\ddot{a}(t)$ imposed on the rigid foundation, and (b) the shock excitation is represented by a force $P(t)$ applied to the rigid mass. For shock excitation of the foundation, the purpose of the isolator is to reduce the magnitude of acceleration $\ddot{x}(t)$ transmitted to the isolated mass whereas, for shock excitation of the isolated mass, the purpose of the isolator is to reduce the magnitude of force $F_T(t)$ transmitted to the foundation. In the latter case, the isolated mass always experiences greater accelerations than it would without the shock isolator present.

Nature of Shock Environments

Shock excitation is generally described by a shock pulse, which specifies the time-history of the acceleration, velocity, displacement or force excitation for the time interval of the applied shock. Service shock conditions may be represented by shock pulses having complex time-histories which are analyzed by numerical analysis techniques or by mathematically modeling the shock environment using relatively simple analytical functions.[1] A variety of mathematical analysis techniques exist for studying dynamics problems involving complex shock excitation; for example, a recent Sound and Vibration article dealt with application of Fourier transforms in the frequency analysis of mechanical shock.[3] Only idealized forms of shock excitation are considered in this article so that attention is focused on the theoretical performance characteristics of isolation systems rather than the mathematical techniques employed in their analysis.
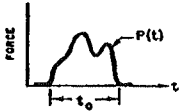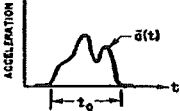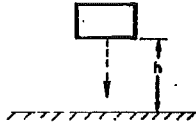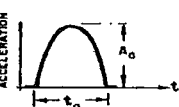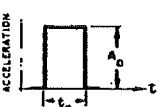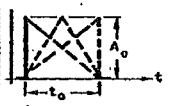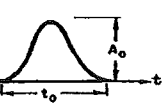
Idealized forms of shock excitation are shown in Table 1. The distinguishing characteristics of the various types of shock excitation include the shape of the shock pulse, the peak magnitude of the shock excitation, and the shock pulse time duration. The velocity change V that occurs as a result of the shock excitation is also presented in Table 1 for each type of shock pulse.

Impulsive Shock. Shock excitation in the form of an applied shock force, which has a high peak magnitude and a time duration that is short relative to the natural period of vibration of the system, is usually defined as impulsive shock, where impulse I is given by

$$I = \int_0^{t_0} P(t)\,dt \qquad (1)$$

and the force $P(t)$ is constant (generally zero) and of equal values before time $t = 0$ and after time $t = t_0$. For an infinitesimally short time duration t_0, the impulsive shock represents an impact condition wherein momentum transfer occurs instantaneously, during which the mass experiences an instantaneous

Table 1 — Idealized forms of shock excitation and the velocity change V associated with each shock pulse.

FORCE IMPULSE	ACCELERATION IMPULSE
$V = \frac{1}{m}\int_0^{t_0} P(t)\,dt$	$V = \int_0^{t_0} \ddot{a}(t)\,dt$
VELOCITY SHOCK $V = V_2 - V_1$	**FREE FALL IMPACT** $V = \sqrt{2gh}$ (inelastic impact) $V = 2\sqrt{2gh}$ (elastic impact)
HALF-SINE ACCELERATION $V = \frac{2g}{\pi} A_0 t_0$	**RECTANGULAR ACCELERATION** $V = g A_0 t_0$
TRIANGULAR ACCELERATION $V = \frac{g}{2} A_0 t_0$	**VERSED-SINE ACCELERATION** $V = \frac{g}{2} A_0 t_0$

velocity change $V = I/m$, where m is the mass of the body on which the impulsive force $P(t)$ acts.

For an acceleration impulse, the velocity change of the foundation is given by the area under the acceleration shock pulse time-history, where the excitation acceleration $\ddot{a}(t)$ is constant (generally zero) and of equal values before time $t = 0$ and after time $t = t_0$.

Velocity Shock. If the excitation velocity undergoes an instantaneous change, the system is subjected to a velocity shock. The system could experience an instantaneous change from one velocity V_1 to another velocity V_2, as illustrated in Table 1. Alternatively, the system could be initially at rest $(V_1 = 0)$ prior to acquiring a velocity V_2. Finally, the system could be experiencing a velocty V_1 prior to being brought to rest $(V_2 = 0)$. The velocity change $V = V_2 - V_1$ is the algebraic difference between the excitation velocity that exists after and before the shock excitation has taken place.

Free Fall Impact. Impact resulting from free fall

in the gravitational field imposes a velocity shock on the falling object when the impact time duration is short relative to the natural periods of vibration of the elements comprising the object. For impact with no rebound, the shock condition is defined as *inelastic impact*, and the velocity change V is equal to the velocity of impact $(2gh)^{1/2}$, where h is the height of free fall and g is the acceleration of gravity. For impact with full rebound, the shock condition is defined as *elastic impact*, and the velocity change V equals twice the impact velocity.[4] The velocity change is presented graphically in Figure 2 as a function of height of free fall for both elastic and inelastic impact conditions. For many practical cases of free fall impact, the velocity change has a value between $(2gh)^{1/2}$ and $2(2gh)^{1/2}$ because of partial rebound.

Acceleration Shock Pulses. Shock excitations for elastic or inelastic impact conditions may be represented by acceleration shock pulses having half-sine, rectangular, triangular or versed-sine shapes. The half-sine and rectangular pulses provide abrupt initiation and termination of the shock excitation. The initiation and termination of the shock excitation for triangular pulses depends on the relative values of the rise time t_r and the shock pulse time duration t_0. The versed-sine shock pulse provides a smooth initiation and termination of the shock excitation. The velocity change V for each shock pulse is determined solely by the peak magnitude of excitation acceleration A_0 and the shock pulse time duration t_0. Mathematical expressions for these idealized shock pulse shapes follow.

Half-Sine Pulse:

$$A(t) = A_0 \sin \pi \, (t/t_0) \quad (0 < t < t_0) \quad (2)$$

Rectangular Pulse:

$$A(t) = A_0 \quad (0 < t < t_0) \quad (3)$$

Triangular Pulses:

$$A(t) = A_0 \left(\frac{1}{t_r/t_0} \right) \left(t/t_0 \right) \quad (0 < t < t_r)$$

$$A(t) = A_0 \left(\frac{1}{1 - t_r/t_0} \right) \left(1 - t/t_0 \right)$$

$$(t_r < t < t_0) \quad (4)$$

where the ratio t_r/t_0 is the fraction of the shock pulse devoted to the rise era. Initial peak sawtooth, symmetrical, and terminal peak sawtooth triangular pulses are obtained by setting t_r/t_0 equal to 0, ½ and 1, respectively.

Versed-Sine Pulse:

$$A(t) = (½) \, A_0 \, [1 - \cos 2\pi(t/t_0)] \quad (0 < t < t_0) \quad (5)$$

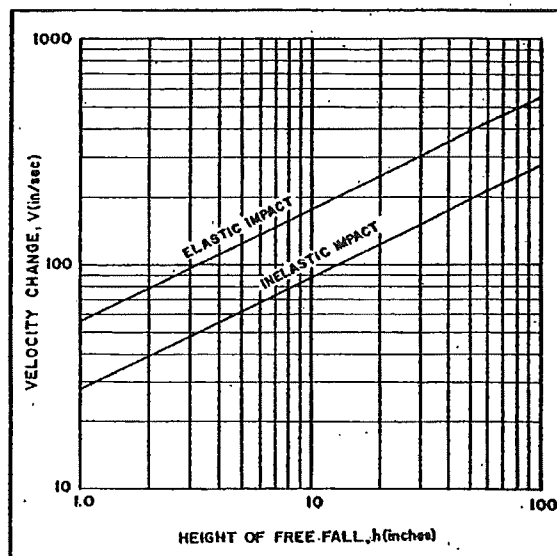Force Shock Pulses. Idealized force shock pulses

Figure 2 — Velocity change imposed on a freely falling body during elastic and inelastic impact [after Crede, Ref. 2].

may be represented by the half-sine, rectangular, triangular and versed-sine pulse shapes presented in Table 1 in terms of acceleration shock pulse excitation. The force time-history $P(t)$ is defined by the mathematical relations for $A(t)$ given by Eqs. (2) to (5) in terms of the peak magnitude of excitation force P_0 (replacing A_0), the shock pulse time duration t_0, and the shock pulse rise time t_r.

Sustained Loading. Sustained loading exists in a dynamic environment when a constant force is applied to the mass and is maintained for an extended length of time, or a constant level of acceleration is imposed upon the foundation and is maintained for an extended length of time. The sustained level of loading may be considered as being reached instantaneously or over a finite time duration, where t_r represents the rise time of the leading edge of the sustained loading time-history.

Conditions of sustained loading are normally categorized as shock because of the sudden manner in which the excitation force or acceleration changes from a reference magnitude to its maximum sustained magnitude of force P_s or acceleration A_s. Examples of typical idealized sustained acceleration time-histories are illustrated in Figure 3, where the onset of sustained acceleration takes place in an instantaneous step in Figure 3(a) and over finite time durations in Figure 3(b)-(d). Since the instantaneous step represents the most abrupt shock condition, it is the type most frequently employed in specifying the sustained loading response characteristics of shock isolation systems. Mathematical expressions for these idealized sustained acceleration time-histories follow.

Instantaneous Step:

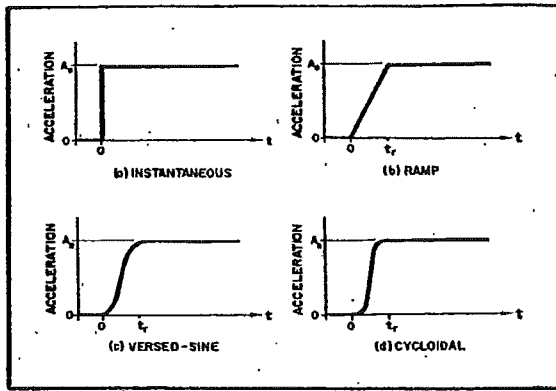$$A(t) = A_s \quad (t > 0) \quad (6)$$

Figure 3 — Sustained acceleration time-histories with typical leading edge characteristics.

Ramp Step:

$$A(t) = A_s(t/t_r) \quad (0 < t < t_r)$$
$$A(t) = A_s \quad (t > t_r) \tag{7}$$

Versed-Sine Step:

$$A(t) = (\tfrac{1}{2}) A_s [1 - \cos \pi (t/t_r)] \quad (0 < t < t_r)$$
$$A(t) = A_s \quad (t > t_r) \tag{8}$$

Cycloidal Step:

$$A(t) = (A_s/2\pi) [2\pi(t/t_r) - \sin 2\pi(t/t_r)]$$
$$(0 < t < t_r)$$
$$A(t) = A_s \quad (t > t_r) \tag{9}$$

Basic Concept of Shock Isolation

Passive shock isolators are resilient elements inserted between the source of shock excitation and the system requiring protection. A reduction in the magnitude of system response is provided because of the ability of the isolator to store energy at the relatively high rate associated with the shock excitation, and subsequently release it at a relatively low rate. Release of the strain energy stored in the isolator causes the isolated body to vibrate at the natural frequency of the isolation system, until the energy is dissipated by the isolator damping mechanism.[5]

The dynamic performance of an undamped passive shock isolation system is illustrated qualitatively in Figure 4 for shock excitation of the foundation. The shock excitation is in the form of an acceleration time-history $\ddot{a}(t)/g$ represented by a pulse of a given shape having a peak magnitude of acceleration A_0 and a time duration t_0. The undamped natural period τ_0 of the isolation system is selected to be a relatively high value compared to the shock pulse time duration t_0, so that the acceleration response $A(t) = \ddot{x}(t)/g$ is represented by a low-frequency transient vibration having a maximum magnitude of acceleration A_{max} that is less than the peak magnitude of shock excitation A_0. The maximum value of the relative displacement $\delta_{max} = (x-a)_{max}$ is also of considerable importance since it determines the

maximum isolator stress and isolation system clearance requirements.

For the case of force excitation of the isolated mass, a passive isolator is introduced to provide a relatively long natural period τ_0 of the isolation system so that the maximum magnitude of force transmitted to the foundation $(F_T)_{max}$ is less than the peak magnitude P_0 of the force time-history $P(t)$, which has a time duration t_0. The maximum value of absolute displacement of the mass X_{max} determines the maximum isolator stress and the isolation system clearance requirements.

Even though isolation of both shock and vibration generally is accomplished by use of low-frequency isolation systems, an isolator that exhibits good vibration isolation does not necessarily provide adequate shock isolation. It is often necessary to employ isolators with nonlinear stiffness characteristics to achieve a satisfactory compromise between shock and vibration isolation requirements. Conditions of sustained loading are of particular importance under these circumstances because they may cause the isolator to bottom or operate in a nonlinear high-stiffness region. In general, therefore, shock and vibration isolation requirements must be considered as joint design criteria.

Static Deflection

Selection of a high value of the isolation system undamped natural period τ_0 is comparable to providing a low undamped natural frequency f_0 which, in units of Hz, is defined as follows

$$f_0 = \frac{1}{\tau_0} = \frac{\omega_0}{2\pi} = \frac{1}{2\pi}\sqrt{\frac{k}{m}} \tag{10}$$

where ω_0 is the undamped circular natural frequency in units of rad/sec, k is the linear stiffness of the isolator, and m is the mass of the isolated body. Large values of *static detection* δ_{st} are associated with low-frequency isolation systems, as indicated by the following relation

$$\delta_{st} = 9.8/f_0^2 \quad (inches) \tag{11}$$

which is presented graphically in Figure 5. Furthermore, increasingly larger dynamic displacements of the isolation system occur for a given shock excitation as the natural frequency is decreased. Consequently, selection of the isolation system natural frequency is made by determining the best compromise between the maximum acceleration (or force) and displacement response magnitudes. Lateral stability and drift characteristics of certain types of low-stiffness passive isolators also influence the selection of natural frequency.

The lowest natural frequency using off-the-shelf commercially available shock isolators generally is in the neighborhood of 5 Hz. Of course, given sufficient space and appropriate means of introduc-
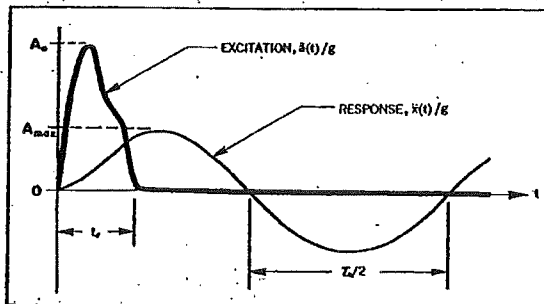
Figure 4 — *Qualitative representation of undamped isolation system performance characteristics for shock excitation of the foundation.*
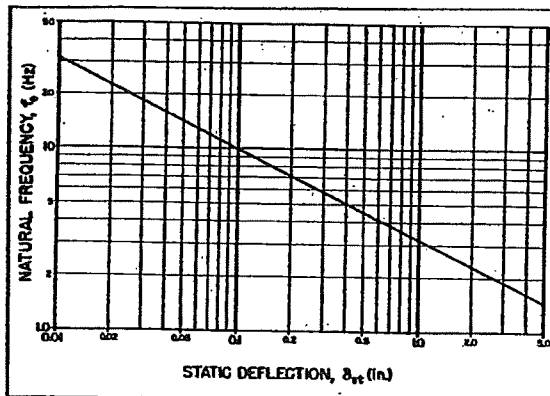

Figure 5 — *Relationship between isolation system static deflection and undamped natural frequency.*
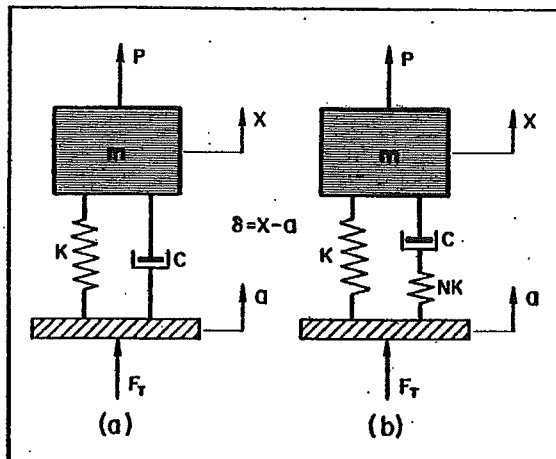

Figure 6 — *Schematic diagrams of viscous damped isolation systems with (a) directly coupled and (b) elastically coupled damping mechanisms.*

ing adequate damping, a lower natural frequency can be achieved by use of large metallic springs, although the sizable static deflection and potential lateral stability problems must be considered. Natural frequencies as low as 0.5 Hz can be provided with zero *static deflection* by use of passive pneumatic isolators that employ an automatic height control

mechanism.[2, 6-8] These isolators may be considered *semi-active* in the sense that power is required to operate a valve which functions to maintain a nominal fixed height of isolator under slow load variations; however, shock and vibration isolation are provided essentially in accordance with the passive stiffness characteristics of the pneumatic isolator.

Equations of Motion

Differential equations of motion for the linear single-mass isolation systems with directly coupled and elastically coupled viscous damping shown in Figure 6(a) and Figure 6(b), respectively, are as follows

$$\ddot{x} + 2\zeta\,\omega_0\,\dot{\delta} + \omega_0^2\,\delta = P/m \qquad (12a)$$

$$\left(\frac{2\zeta}{N\omega_0}\right)\dddot{x} + \ddot{x} + 2\zeta\omega_0\left(\frac{N+1}{N}\right)\dot{\delta}$$
$$+ \omega_0^2\,\delta = P/m + \left(\frac{2\zeta}{N\omega_0}\right)\dot{P}/m$$
$$(12b)$$

where x is the absolute displacement of the isolated mass, $\delta = (x\text{-}a)$ is the relative displacement across the isolator, and the shock excitation is assumed to be specified by the force P, the foundation displacement a, or time-derivatives of a. The viscous damping ratio $\zeta = C/C_G$ is the ratio of the viscous damping coefficient C to the critical value of viscous damping $C_G = 2\,(k\ m)^{1/2}$ for $N = \infty$, and the stiffness ratio N is the ratio of the damper elastic coupling stiffness to the main load-carrying stiffness. The directly coupled viscous damped system shown in Figure 6(a) is the mathematical model traditionally used by vibration engineers to study the effects of damping; however, the elastically coupled viscous damped system, or variations thereof, shown in Figure 6(b) has been demonstrated to be a mathematical model that more accurately portrays the dynamic characteristics of linear shock and vibration isolation systems.[9] The system with directly coupled damping is observed to be a degenerate case of the system with elastically coupled damping wherein the stiffness ratio N equals infinity.

Dimensionless Response Parameters

The maximum magnitude of isolation system response parameters, such as A_{max} and δ_{max} for shock excitation of the foundation and $(F_T)_{max}$ and X_{max} for shock excitation of the isolated mass, are generally of primary interest. However, it frequently is convenient to present the performance characteristics of shock isolation systems in terms of two dimensionless response parameters — the *shock transmissibility* T_s and the *shock amplification factor* H_s.

Shock Pulse Excitation. For shock excitation of the foundation, the shock transmissibility T_s and the shock amplification factor H_s are defined as follows

$$T_s = \frac{A_{max}}{A_0} \quad (13)$$

$$H_s = \frac{\delta_{max}}{\Delta_{st}} \quad (14)$$

where the *equivalent static deflection* Δ_{st} is given by

$$\Delta_{st} = A_0 g / \omega_0^2 \quad (15)$$

The corresponding definitions for shock force excitation of the isolated mass are as follows

$$T_s = \frac{(F_T)_{max}}{P_0} \quad (16)$$

$$H_s = \frac{X_{max}}{\Delta_{st}} \quad (17)$$

$$\Delta_{st} = P_0 / k \quad (18)$$

where the force transmitted to the foundation is given by $F_T = C\dot{X} + kX$ for directly coupled viscous damping and by $\dot{F}_T + (Nk/C)F_T = k(N + 1)\dot{X} + (Nk^2/C)X$ for elastically coupled viscous damping. The equivalent static deflection Δ_{st} is that deflection which would result if the peak magnitude of shock excitation (A_0 or P_0) were applied statically to the isolated mass.

Sustained Loading. For sustained acceleration of the foundation, the shock transmissibility T_s and the shock amplification factor H_s are defined as follows

$$T_s = \frac{A_{max}}{A_s} \quad (19)$$

$$H_s = \frac{\delta_{max}}{\Delta_{st}} \quad (20)$$

where

$$\Delta_{st} = A_s g / \omega_0^2 \quad (21)$$

The corresponding definitions for a sustained force applied to the isolated mass are as follows

$$T_s = \frac{(F_T)_{max}}{P_s} \quad (22)$$

$$H_s = \frac{X_{max}}{\Delta_{st}} \quad (23)$$

$$\Delta_{st} = P_s / k \quad (24)$$

The equivalent static deflection Δ_{st} is that deflection which would result if the sustained magnitude of shock excitation (A_s or P_s) were applied statically to the isolated mass.

Linear Isolation Systems. Certain equalities exist among the dimensionless response parameters for linear isolation systems. For *shock pulse excitation*, the shock transmissibility expression given by Eq. (13) also represents the ratio of appropriate response and excitation parameters for velocity or dis-

placement shock excitation of the foundation. Furthermore, the shock transmissibility expressions given by Eqs. (13) and (16) are equal, as are the shock amplification factor expressions given by Eqs. (14) and (17), as follows

$$T_s = \frac{A_{max}}{A_0} = \frac{\dot{X}_{max}}{\dot{a}_0} = \frac{X_{max}}{a_0} = \frac{(F_T)_{max}}{P_0} \quad (25)$$

$$H_s = \frac{\delta_{max}}{A_0 g / \omega_0^2} = \frac{X_{max}}{P_0/k} \quad (26)$$

where $\dot{a}_0$ and a_0 are the peak magnitudes of velocity and displacement shock pulses, respectively.

For *sustained loading conditions*, the shock transmissibility expression given by Eq. (19) also represents the ratio of appropriate response and excitation parameters for sustained velocity or displacement of the foundation. Also, the shock transmissibility expressions given by Eqs. (19) and (22) are equal, as are the shock amplification factor expressions given by Eqs. (20) and (23), as follows

$$T_s = \frac{A_{max}}{A_s} = \frac{\dot{X}_{max}}{\dot{a}_s} = \frac{X_{max}}{a_s} = \frac{(F_T)_{max}}{P_s} \quad (27)$$

$$H_s = \frac{\delta_{max}}{A_s g / \omega_0^2} = \frac{X_{max}}{P_s/k} \quad (28)$$

where $\dot{a}_s$ and a_s are the values of sustained velocity and displacement imposed on the foundation, respectively.

Effect of Damping. For zero damping, the shock transmissibility T_s and the shock amplification factor H_s are equal since $\ddot{X}_{max} = gA_{max} = -\omega_0^2 \delta_{max}$ and $(F_T)_{max} = kX_{max}$ for shock excitation of the foundation and of the isolated mass, respectively. Hence, for *linear* shock isolation systems with *zero damping*, the following relationship applies

$$T_s = H_s \quad (\zeta = 0) \quad (29)$$

In the presence of damping, the maximum acceleration response A_{max} is not directly proportional to the maximum relative displacement response δ_{max} and $(F_T)_{max}$ is not directly proportional to X_{max}. Therefore, the shock transmissibility in general does *not* equal the shock amplification factor[10] although, for small directly coupled damping ($\zeta < 0.2$), the relationship of Eq. (29) is approximately true. This fact is clearly demonstrated later in the article by the design graphs for T_s and H_s that are provided for a wide range of values of viscous damping ratio ζ.

Erroneous information on the effect of damping has appeared in the technical literature due to improper adaptation of amplification factor data presented by Mindlin and his co-workers [11, 12] for half-sine acceleration pulse shock excitation. When the *amplification factor* data are reproduced and re-labeled as *shock transmissibility*[13] or *dynamic load factor*,[14] Eq. (29) has been tacitly assumed to apply and, for values of damping other than zero, the

7

results are incorrect. Similar erroneous results are obtained when using the generalized excitation and response notation employed by Ayre.[15] However, Marous and Schell[16, 17] have made proper distinction between the generalized response parameters for undamped and damped systems.

Extensive analytical results showing the effect of viscous damping on the shock response for acceleration pulse shock excitation has been given by Luke[18] for directly coupled damping and by Derby and Calcaterra[19] for elastically coupled damping. Similar information for displacement pulse shock excitation has been given by Snowdon.[20] The effect of nonlinear damping on the shock response of isolation systems is a considerably more complex problem, for which general analytical methods,[21] graphical techniques, [15, 22, 23] and results presented in the form of shock spectra[24] are available.

Velocity Shock Isolation With Zero Damping

In the absence of damping, an instantaneous velocity change V gives rise to acceleration, force and displacement responses that are sinusoidal time-histories, as shown in Figure 7(a). The maximum response magnitudes are given by

$$A_{max} \text{ or } \frac{(F_T)_{max}}{mg} = \frac{V\omega_0}{g} = 2\pi f_0 V/g \quad (30)$$

$$\delta_{max} \text{ or } X_{max} = V/\omega_0 = V/2\pi f_0 \quad (31)$$

Values of A_{max} and δ_{max} are presented in Figure 8 for a wide range of values of velocity change V (in/sec) and natural frequency $f_0(Hz)$. For a given value of V, this graph provides a means of selecting the isolation system natural frequency to achieve a satisfactory compromise between the maximum acceleration and relative displacement response magnitudes. For velocity shock (force impulse) excitation of the isolated mass, the parameters A_{max} and δ_{max} determined from Figure 8 represent $(F_T)_{max}/mg$ and X_{max}, respectively.

Velocity Shock Isolation With Viscous Damping

The presence of damping can materially affect isolation system response characteristics. The addition of a small amount of viscous damping will reduce the acceleration or force response; however, an excessive degree of damping can cause the acceleration or force response to be increased over that which exists for zero damping. Values of optimum damping for minimax response (minimized maximum response magnitudes) can be determined for various optimum performance criteria to form the basis for establishing preferred ranges of isolator damping.

Directly Coupled Damping. For an isolation system with directly coupled viscous damping, as shown in Figure 6(a), the acceleration, force and displacement responses are exponentially decaying sinusoidal
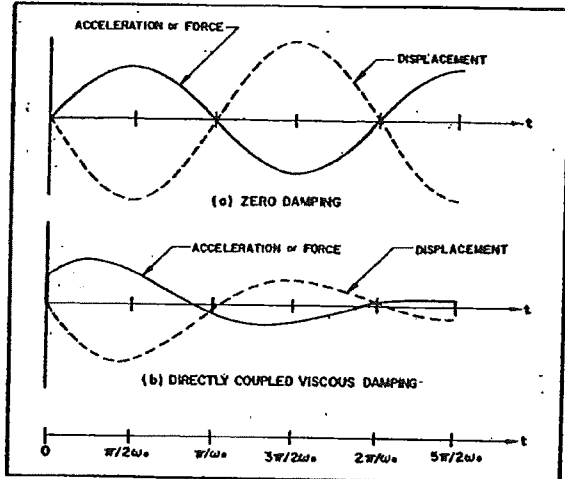

Figure 7 — Response time-histories for velocity shock excitation of (a) undamped and (b) directly coupled viscous damped isolation systems.
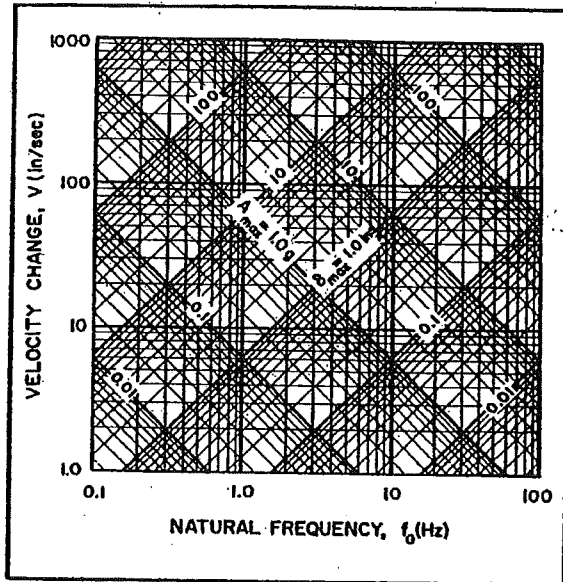

Figure 8 — Undamped isolation system response maxima for velocity shock excitation of the foundation. For velocity shock excitation of the isolated mass, A_{max} and δ_{max} represent $(F_T)_{max}/mg$ and X_{max}, respectively.

time-histories, as illustrated in Figure 7(b). Upon application of the velocity shock at time $t = 0$, the acceleration A (or force F_T) instantaneously acquires magnitude given by

$$A(o) \text{ or } \frac{F_T(o)}{mg} = 2\zeta V\omega_0/g \quad (32)$$

whereas the displacement δ (or X) initially has a zero magnitude as in the case of zero damping. Since the value of response acceleration $A(o)$ given by Eq. (32) is acquired instantaneously, the initial value of the jerk of the isolated mass $\ddot{X}(o)$ is infinite. For $\zeta < 0.5$, the initial acceleration or force response
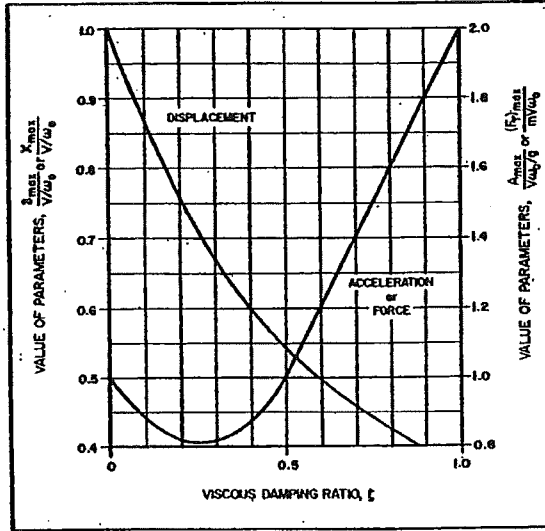
SOUND AND VIBRATION •

Figure 9 — *Acceleration or force and displacement response maxima for isolation system with directly coupled viscous damping subjected to velocity shock excitation [after Mindlin, Ref. 11].*

is less than the maximum value ultimately achieved whereas, for $\zeta > 0.5$, the initial value of acceleration or force response is the maximum magnitude attained, and the magnitude of response decreases thereafter.[11]

Variation of the maximum magnitudes of acceleration, force and displacement, normalized with respect to the magnitudes that exist for zero damping, are presented graphically in Figure 9 as a function of the viscous damping ratio ζ. For values of viscous damping in the range $0 < \zeta < 0.5$, the maximum acceleration or force response is below that which exists for zero damping whereas, for $\zeta > 0.5$ the maximum response is greater and increases in direct proportion to ζ. For all values of the viscous damping ratio, the maximum displacement response magnitudes are decreased below those that exist for zero damping.

The dimensionless acceleration or force response parameters are minimized when the viscous damping ratio has the value $\zeta = 0.26$. For a specified value of natural frequency ω_0 (based, for example, on static deflection considerations) and an optimum value of viscous damping ratio $\zeta_{op} = 0.26$, the maximum acceleration or force response magnitude is reduced 19 percent below the corresponding value for zero damping, as follows.

$$(A_{max})_{op} \text{ or } \left[\frac{(F_T)_{max}}{mg}\right]_{op} = 0.81 V\omega_0/g$$

$$(\zeta_{op} = 0.26) \tag{33}$$

and the resulting maximum displacement response magnitude is

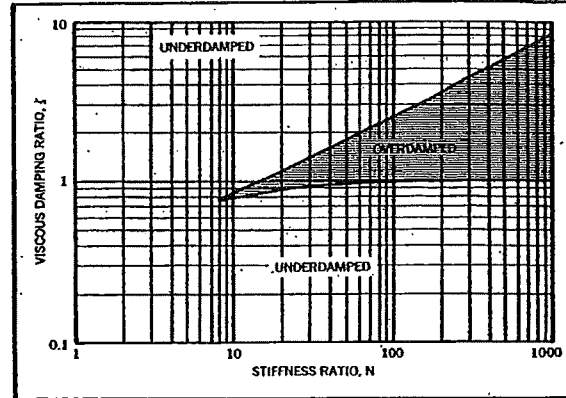$$\delta_{max} \text{ or } X_{max} = 0.7V/\omega_0 \tag{34}$$

Figure 10 — *Regions of underdamping and overdamping for an isolation system with elastically coupled viscous damping [after Derby and Calcaterra, Ref. 19].*

which represents a 30 percent reduction below that which exists for zero damping.

A more general optimum performance criterion involves determination of the amount of damping and the value of natural frequency that minimizes the maximum acceleration or force response magnitudes for a *specified* maximum magnitude of displacement response.[19] In this case, an optimum value of viscous damping ratio $\zeta_{op} = 0.4$ and an optimum natural frequency given by

$$(\omega_0)_{op} = 0.6V/\delta_{max} \tag{35}$$

result in minimizing the maximum acceleration or force magnitude, as follows:

$$(A_{max})_{op} \text{ or } \left[\frac{(F_T)_{max}}{mg}\right]_{op} = \frac{0.52V^2}{g\delta_{max}} \text{ or } \frac{0.52V^2}{gX_{max}}$$

$$(\zeta_{op} = 0.4) \tag{36}$$

An alternative statement of this optimum performance criterion is that, for a selected maximum magnitude of acceleration response A_{max} (or force response $(F_T)_{max}$), the resulting maximum magnitude of displacement response δ_{max} (or X_{max}) is minimized when $\zeta = 0.4$ and the natural frequency ω_0 is determined according to Eq. (35). Comparison of this optimum damped system with the "best possible" or "ideal" theoretical solution, which involves the use of a constant-force energy dissipating device (e.g., dry-friction damper or a crushable material), indicates that, for a specified velocity change and maximum displacement response, the maximum acceleration response is only 4 percent higher than that for the "best possible" shock isolation system.[19] However, a passive constant-force device may not return to its initial position subsequent to the shock excitation, whereas an isolator comprised of a spring and an optimum viscous damper does.

For those cases where high-frequency vibration isolation is an important design criterion, a value of $\zeta = 0.4$ may be too high because of excessive de-
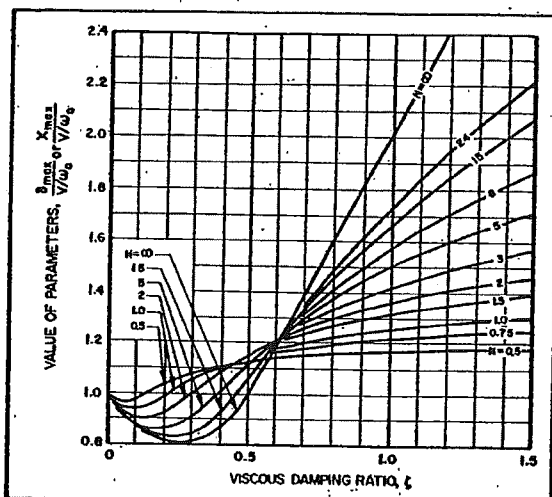
Figure 11 — Acceleration or force response maxima for an isolation system with elastically coupled viscous damping subjected to velocity shock excitation [after Derby and Calcaterra, Ref. 19].
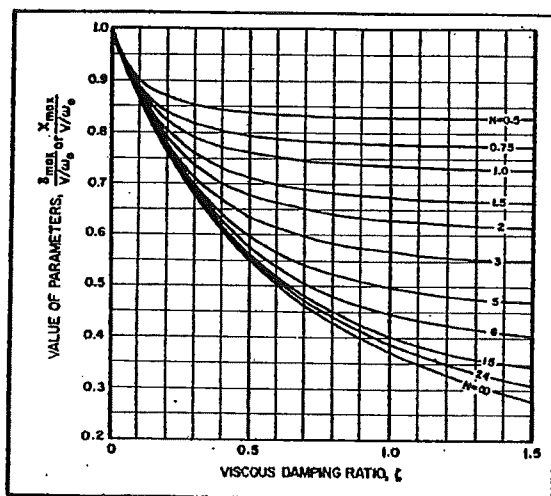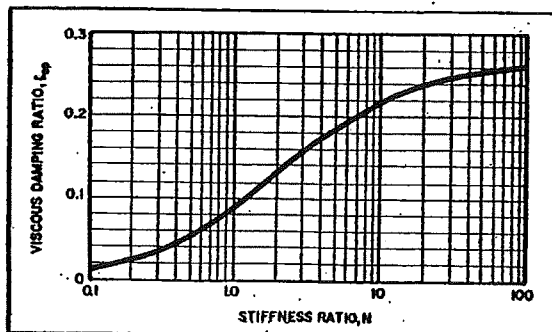

Figure 12 — Displacement response maxima for an isolation system with elastically coupled viscous damping subjected to velocity shock excitation [after Derby and Calcaterra, Ref. 19].

Figure 13 — Optimum viscous damping ratio for an isolation system with elastically coupled viscous damping and a specified value of natural frequency ω_0 [after Derby and Calcaterra, Ref. 19].

gradation of vibration isolation at high frequencies. Also, the static deflection associated with the optimum natural frequency $(\omega_0)_{op}$ may be greater than desired. Consequently, for most practical problems, a value of viscous damping ratio should be selected in the range $0.1 < \zeta < 0.4$ for velocity shock excitation of an isolation system with directly coupled viscous damping.

Elastically Coupled Damping. For an isolation system with elastically coupled viscous damping, as shown in Figure 6(b), the acceleration, force and displacement responses are represented by complex solutions of a third-order differential equation and generally appear to be exponentially decaying harmonic time-histories. Due to the presence of the damper elastic coupling stiffness Nk, both the acceleration A (or force F_T) and displacement δ (or X) initially have zero magnitudes upon application of the velocity shock at time $t = 0$. Hence, the initial jerk of the isolated mass $\ddot{X}(o)$ is finite as it is for zero damping.

For values of the stiffness ratio $N < 8$, the isolation system is underdamped for all values of damping; that is, the response motion is oscillatory. For values of $N > 8$, there are two values of the viscous damping ratio ζ for which the system is critically damped, and the system is overdamped (non-oscillatory response motion) for damping between these two values.[19] The regions of underdamping and overdamping for a wide range of values of the viscous damping ratio ζ and the stiffness ratio N are illustrated in Figure 10. For values of $\zeta < 0.77$, the isolation system with elastically coupled viscous damping is always underdamped and experiences oscillatory response motions.

Variation of the maximum magnitudes of acceleration, force and displacement, normalized with respect to the magnitudes that exist for zero damping, are presented in Figures 11 and 12 as a function of the viscous damping ratio ζ and the stiffness ratio N. Referring to Figure 11, for sufficiently low values of damping the maximum acceleration or force response magnitude can be reduced below that which exists for zero damping whereas, for $\zeta > 0.5$, the maximum response is always greater, and the dimensionless acceleration or force response parameter approaches $(N + 1)^{1/2}$ as the viscous damping ratio approaches infinity. For all values of the viscous damping ratio, the maximum displacement response magnitude is decreased below that which exists for zero damping, as shown in Figure 12, and the dimensionless displacement response parameter approaches $1/(N + 1)^{1/2}$ as the viscous damping ratio approaches infinity.

For specified values of natural frequency ω_0, there is an optimum value of damping ζ_{op} that minimizes the maximum acceleration or force response magnitude, as shown graphically in Figure 13 as a function of the stiffness ratio N. For this optimum perfor-
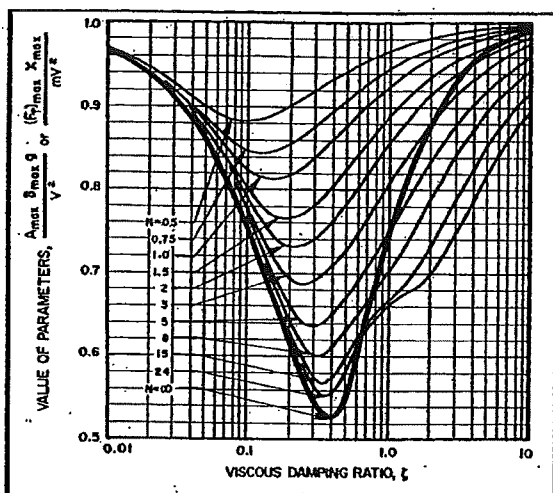
SOUND AND VIBRATION •

10

Figure 14 — *Generalized acceleration or force and displacement response maxima for an isolation system with elastically coupled viscous damping subjected to velocity shock excitation [after Derby and Calcaterra, Ref. 19].*
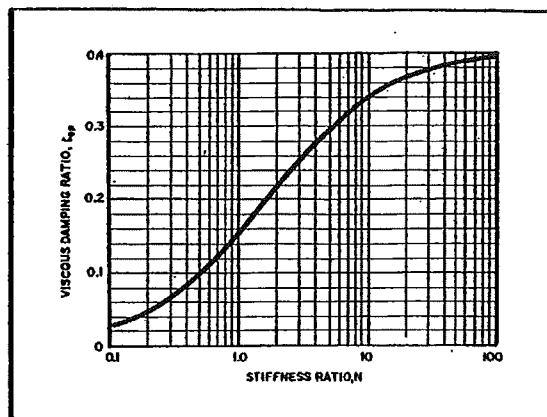

Figure 15 — *Optimum viscous damping ratio for an isolation system with elastically coupled viscous damping having a minimax response corresponding to the minimum of the generalized response maxima curves presented in Fig. 14 [after Derby and Calcaterra, Ref. 19].*
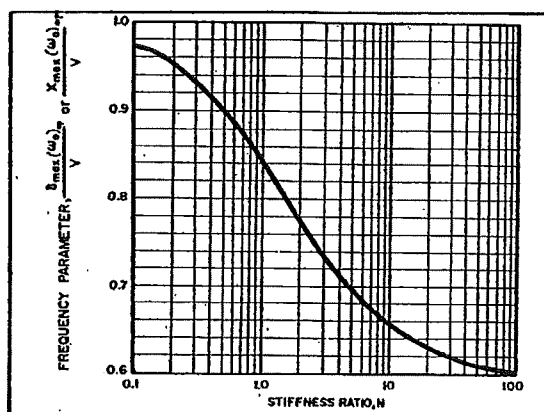

Figure 16 — *Frequency parameter providing the value of the optimum natural frequency $(\omega_o)_{op}$ for an isolation system with elastically coupled viscous damping and a value of optimum viscous damping ratio specified in Fig. 15 [after Derby and Calcaterra, Ref. 19].*

mance criterion, the optimum viscous damping ratio has a value in the range $0 < \zeta < 0.26$, where $\zeta_{op} = 0.26$ applies for $N = \infty$ corresponding to the directly coupled viscous damping mechanism.

The more general optimum performance criterion, which involves determination of the amount of damping and the value of the natural frequency that minimizes the maximum acceleration or force magnitudes for a *specified* maximum magnitude of displacement response, cannot be solved analytically in closed form. However, numerical search techniques can be employed to determine the influence of the three design parameters ζ, ω_0 and N on the optimum response for velocity shock excitation.[19] By eliminating the natural frequency ω_0 from the search procedure, graphical design data for the parameter $A_{max} \delta_{max} g/V^2$ or $(F_T)_{max} X_{max}/mV^2$ can be developed, as shown in Figure 14. This design graph essentially represents the product of the abscissa quantities of Figures 11 and 12, which excludes the effect of the natural frequency ω_0. Having arrived at an acceptable combination of maximum acceleration or force and displacement response magnitudes from Figure 14 by selecting appropriate values of the viscous damping ratio ζ and the stiffness ratio N, the required natural frequency can be determined from Figures 11 or 12 in terms of the parameters A_{max} or $(F_T)_{max}$ and δ_{max} or X_{max}, respectively.

Values of the optimum viscous damping ratio ζ_{op} that correspond to the minimum values of the response curves presented in Figure 14 are shown as a function of the stiffness ratio N in Figure 15. The parameter ζ_{op} has a value in the range $0 < \zeta < 0.4$, where $\zeta_{op} = 0.4$ applies for $N = \infty$ corresponding to the directly coupled viscous damping mechanism. The optimum natural frequency $(\omega_0)_{op}$ that is associated with each value of ζ_{op} may be determined

from the optimum frequency parameter, which is presented graphically in Figure 16 as a function of the stiffness ratio N, and the maximum displacement response magnitude δ_{max} or X_{max}.

When combined with previously published data for optimization of damping for harmonic vibration excitation[9, 25] the response data presented for velocity shock excitation provides the basis for selecting design parameters to achieve satisfactory isolation characteristics for both shock and vibration excitation.

The response characteristics for shock pulse excitation and sustained loading, and the effect of isolator nonlinear stiffness characteristics, are discussed in the second part of the article to be published in the September 1970 issue of *Sound and Vibration*. A complete list of references will accompany the concluding part of the article.

Passive Shock Isolation · Part II

A discussion of the nature of shock environments, the basic concept of shock isolation, equations of motion, and dimensionless response parameters were discussed in the first part of the article published in the August 1970 issue of *Sound and Vibration*. Isolation system performance characteristics for velocity shock excitation were also presented, including the effect of directly coupled and elastically coupled viscous damping.

The second part of the article is concerned with the response characteristics for shock pulse excitation and sustained loading, including the effect of viscous damping. The article concludes with a discussion of the effect of isolator nonlinear stiffness characteristics and a listing of references for both Parts I and II.

Response for Shock Pulse Excitation

The first complete discussion of the response of a simple mechanical system to shock pulse excitation was presented in Mindlin's monograph on package cushioning.[11] This work was later extended by Jacobsen and Ayre[26] to include a wider variety of shock pulse shapes. Collections of data on the shock response of linear single-degree-of-freedom systems for a wide range of pulse shapes are available in the technical literature, including the effects of viscous damping[10-20,22,26,27], although one must be cautious of shock transmissibility data that has been derived from shock amplification factor data when damping is present, as previously discussed in this article.

The Shock Spectrum Concept. In evaluating the effect of shock pulse shape on the dynamic response of linear isolation systems, the shock spectrum concept is usually employed.[10,28] Basically, a *shock spectrum* is a description of the manner in which the response maxima of single-degree-of-freedom systems vary with natural frequency and damping for a given shock excitation. The most common means of graphically presenting shock spectra is the four-coordinate logarithmic graph paper illustrated in Figure 17. For shock excitation of the foundation, the values of acceleration and displacement provided by Figure 17 correspond to A_{max} and δ_{max}, respectively, whereas, for shock excitation of the isolated mass, the acceleration and displacement values correspond to $(F_T)_{max}/mg$ and X_{max}, respectively.

Complex shock excitations are analyzed by analog or digital computation means to obtain a plot of the shock spectrum. For a given allowable maximum acceleration or force, the required isolation system natural frequency and the resulting maximum relative displacement is obtained directly from the shock spectrum curve. An optimum design can be attained by selecting various values of natural frequency until the best compromise between the maximum
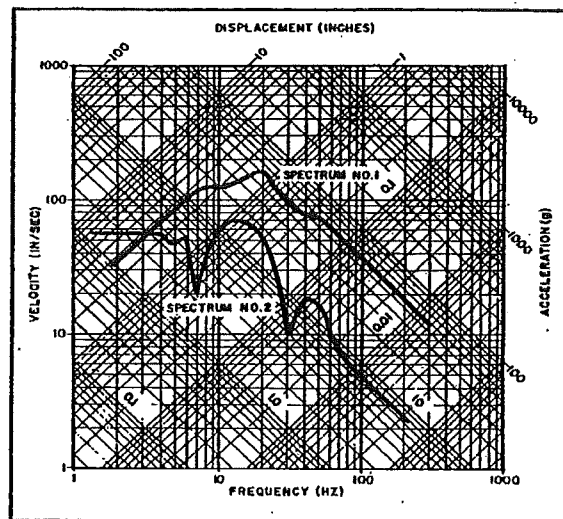

Figure 17 — Four-coordinate logarithmic shock spectrum presentation, with examples of spectra for two shock pulses.

response magnitudes of acceleration or force and displacement is obtained.

Two examples of shock spectra are included in Figure 17 for particular values of damping. For Spectrum No. 1, considering the maximum allowable acceleration response to be 10 g's indicates that a 6 Hz isolation system natural frequency is required, for which the dynamic displacement δ_{max} is 2.7 inches and the static deflection δ_{st} is 0.3 inches. However, if the maximum allowable acceleration is increased to 20 g's, a 10 Hz natural frequency can be employed, for which $\delta_{max} = 2$ inches and $\delta_{st} = 0.1$ inches. Finally, no isolation is needed if the maximum allowable acceleration is increased to 60 g's.

The valleys in Spectrum No. 2 provide potential optimum solutions to the shock isolation problem. A 7 Hz natural frequency will reduce the transmitted acceleration to 2.3 g's, with a dynamic displacement of 0.45 inches and a static deflection of 0.2 inches. However, by allowing 5 g's acceleration to be transmitted, a 30 Hz natural frequency system can be employed, which reduces the dynamic displacement and the static deflection to 0.05 inches and 0.01 inches, respectively. Such "tailored" optimum solutions, of course, require that the nature of the shock excitation does not materially change from one shock occurrence to the next.

Response Characteristics for Zero Damping. The technical literature contains considerable information on the undamped shock spectra for analytically defined pulses, including rectangular, half-sine, versed-sine and triangular shapes. For positive value shock pulses ($\ddot{a}, P > 0$) having a single peak of magnitude
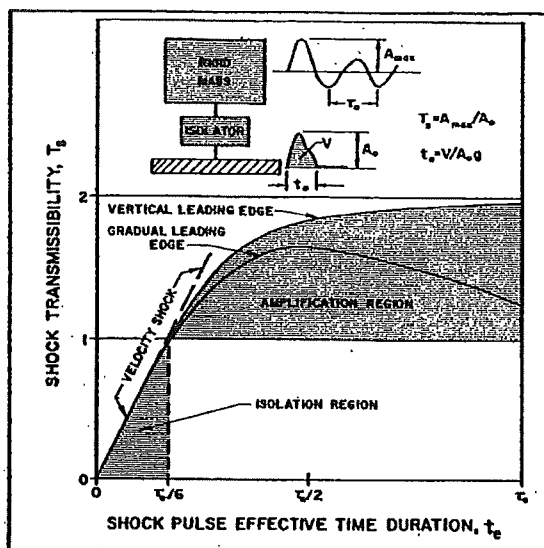
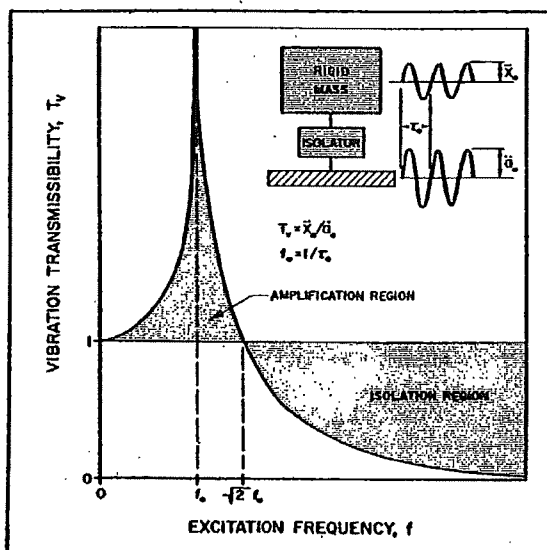Figure 18 — Qualitative representation of shock transmissibility for an undamped linear isolation system.

Figure 19 — Qualitative representation of vibration transmissibility for an undamped linear isolation system.
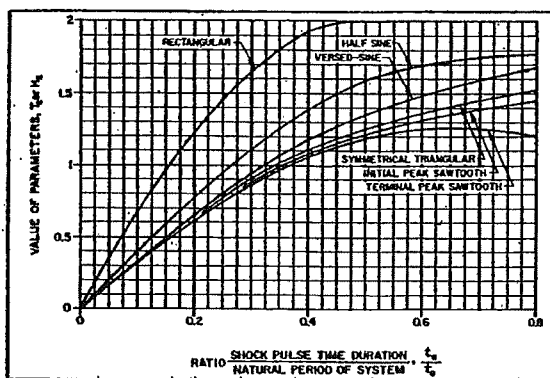

Figure 20 — Shock transmissibility and shock amplification factor for an undamped isolation system subjected to excitation in the form of various shock pulse shapes.

A_0 or P_0, a relatively simple design criteria for shock isolation with zero damping can be established by defining the shock pulse effective time duration t_e, as follows:[13]

$$t_e = \frac{V}{A_0 g} \text{ or } \frac{V}{P_0/m} \qquad (37)$$

For a rectangular pulse, the effective time duration t_e equals the actual pulse duration t_0; however, for all other pulse shapes, the effective time duration is less than the actual pulse time duration. For example, $t_e = (2/\pi)t_0$ for the half-sine pulse, and $t_e = t_0/2$ for the versed-sine and triangular pulses.

A qualitative graphical presentation of shock transmissibility for an undamped linear isolation system is presented in Figure 18. The shock transmissibility curves indicate that amplification of shock occurs for high values of the shock pulse effective time duration, and isolation of shock occurs for effective time durations t_e less than approximately one-sixth the isolation system natural period τ_0. The shape of the shock pulse is unimportant in the shock isolation region and, for all practical purposes, velocity shock conditions apply to the entire isolation region. Therefore, in order to provide isolation of shock, the natural frequency is selected so that $f_0 < 1/6 \cdot t_e$. The shock transmissibility curve presented in Figure 18 is analogous to the transmissibility curve for an undamped linear isolation system subjected to harmonic vibration excitation, as shown in Figure 19, which indicates that amplification of vibration occurs for low values of excitation frequency and isolation of vibration occurs for excitation frequencies greater than $(2)^{1/2}$ times the isolation system natural frequency f_0. In order to provide isolation of vibration, the natural frequency of the isolation system f_0 is made less than 0.7 times the excitation frequency.

The isolation system response depends solely on the velocity change for low values of t_e, on the shock pulse shape and its peak magnitude for intermediate value of t_e, and solely on the peak magnitude of the shock pulse for high values of t_e. The shock transmissibility is directly proportional to the ratio t_e/τ_0 for $t_e < \tau_0/6$. In the range $\tau_0/6 < t_e < 1.5 \tau_0$, the shock transmissibility generally has a value between 1.2 and 2, depending on the shape of the shock pulse. For shock pulses having a leading edge with a gradual rise, the maximum shock transmissibility occurs in the region $\tau_0/3 < t_e < 2 \tau_0/3$ and, for $t_e > 1.5 \tau_0$, the shock transmissibility ranges between 1.0 and 1.2 regardless of the shape of the excitation shock pulse. For shock pulses having a vertical leading edge, the maximum shock transmissibility generally approaches a maximum value of 2 for values of $t_e \geq \tau_0/2$.
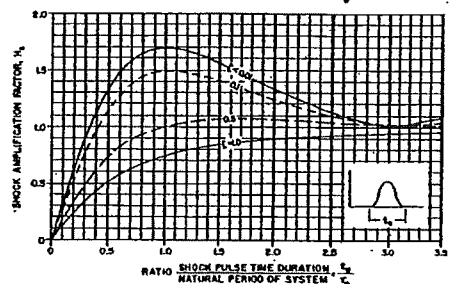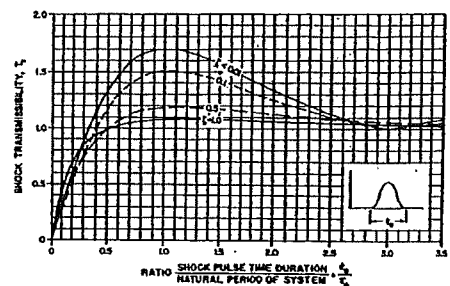
Values of shock transmissibility T_s and shock amplification factor H_s for zero damping are presented in Figure 20 in terms of the relative values of the actual shock pulse time duration t_0 and the isolation system natural period τ_0 for rectangular,
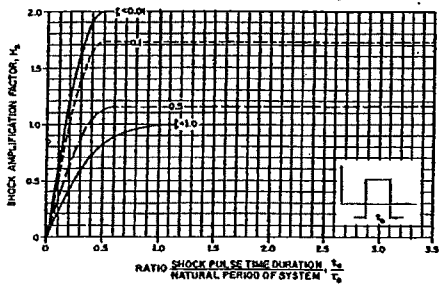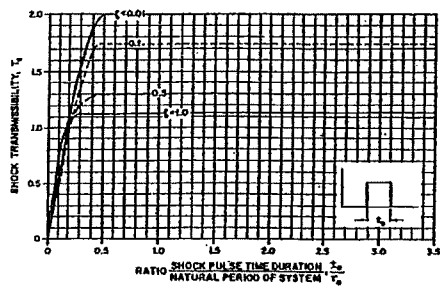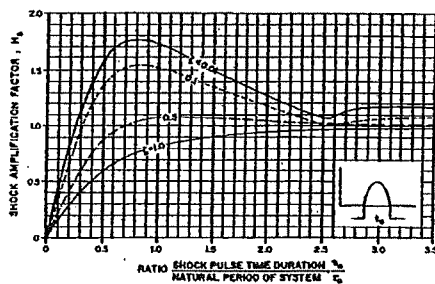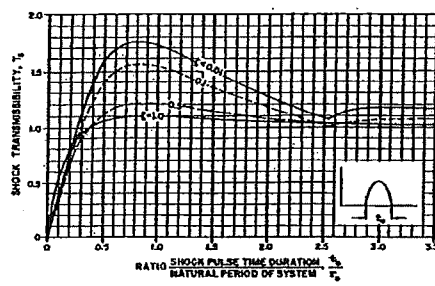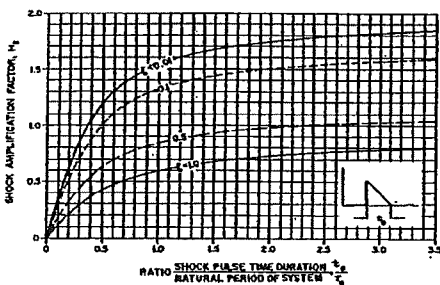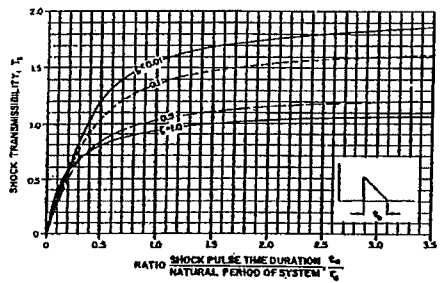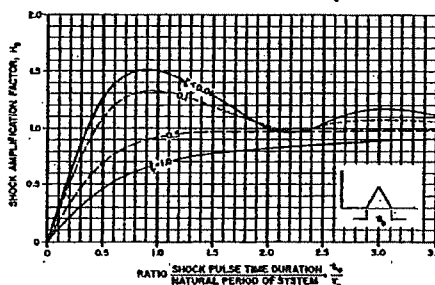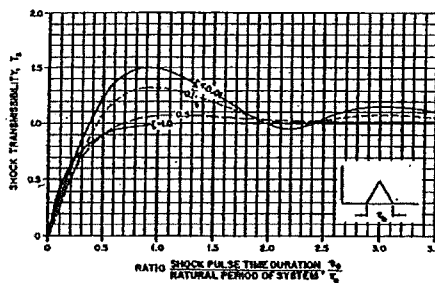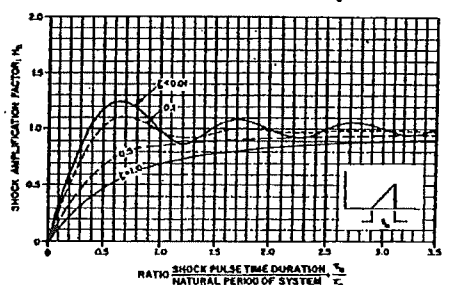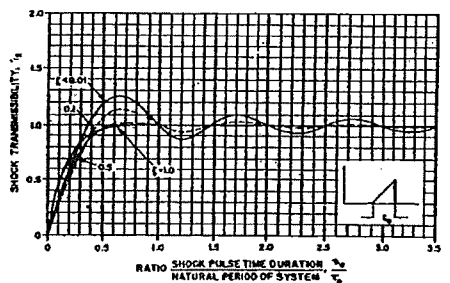
Figure 21 — Shock transmissibility and shock amplification factor for an isolation system with directly coupled viscous damping subjected to (a) rectangular, (b) half-sine, (c) versed-sine, (d) initial peak sawtooth, (e) symmetrical triangle and (f) terminal peak sawtooth pulses [after Luke, Ref. 18].

half-sine, versed-sine and triangular shock pulses. Velocity shock conditions prevail, with less than approximately ten percent overestimate in response prediction, when $t_0 < \tau_0/4$ for a rectangular pulse and $t_o < \tau_0/3$ for half-sine, versed-sine and triangular pulses. For these conditions, relatively simple expressions for shock transmissibility and shock amplification factor exist, as summarized in Table 2.

Effect of Damping. The effect of directly coupled viscous damping on the shock transmissibility T_s and the shock amplification factor H_s for rectangular, half-sine, versed-sine and triangular (initial peak sawtooth, symmetrical, and terminal peak sawtooth) shock pulses is shown in Figure 21.[18] These curves provide values of T_s and H_s defined by Eqs. (25) and (26) as a function of the ratio of shock pulse time duration t_0 to the isolation system natural period τ_0, for various values of the viscous damping ratio ζ. The curves for $\zeta = 0$ and $\zeta = 0.01$ are the same to within approximately a two percent error. For $\zeta < 0.5$ and $t_0/\tau_0 < 1/4$, or any value of ζ and $t_0/\tau_0 > 1/4$, damping has the general effect of reducing both the shock transmissibility and the shock amplification factor. For $\zeta > 0.5$ and $t_0/\tau_0 < 1/4$, the shock transmissibility is greater than that for zero damping while a further decrease in the value of the shock amplification factor results. The isolator essentially acts as a rigid connection between the mass and the foundation for extremely high values of damping, thereby causing the shock transmissibility to approach unity and the shock amplification factor to approach zero for all values of the ratio t_0/τ_0.

Shock response curves similar to those presented in Figure 21 have been developed for elastically coupled viscous damping.[19] The effect of nonlinear damping on the shock response of isolation systems is a considerably more complex problem, for which general analytical methods,[21] graphical techniques[15,22,23] and results presented in the form of shock spectra[24] are available.

Response for Sustained Loading

For conditions of sustained acceleration or force, the isolation system response is a function of the leading edge characteristics of the sustained loading time-history and the isolation system natural period τ_0. Values of shock transmissibility T_s or shock amplification factor H_s for zero damping are pre-
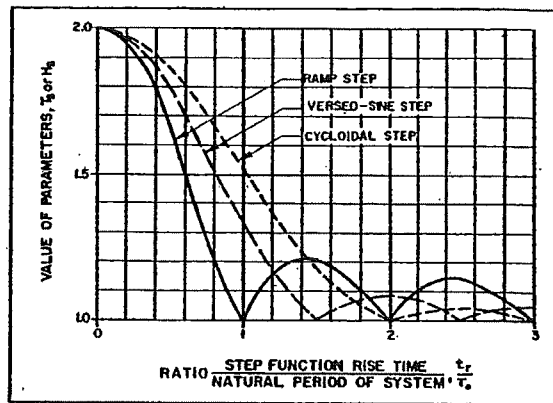

Figure 22 — Shock transmissibility and shock amplification factor for an undamped isolation system subjected to sustained loading with various leading edge characteristics [after Jacobsen and Ayre, Ref. 22 and 26].

sented in Figure 22 for ramp, versed-sine and cycloidal step functions in terms of the ratio of the step function rise time t_r to the natural period of the isolation system τ_0.[15,22,26]

For an instantaneous step $(t_r/\tau_0 = 0)$, T_s and H_s have a value of 2.0, indicating that the response maxima are twice the magnitudes that would result if the sustained loading were applied statically to the mass. For non-zero values of the time ratio t_r/τ_0, the shock transmissibility or shock amplification factor always have a value less than 2.0. The shape of the leading edge characteristic determines the degree of shock transmission, with no amplification (zero overshoot) resulting for certain values of t_r/τ_0 for which T_s and H_s have values of unity; for example, this is the case when $t_r/\tau_0 = 1, 2, 3$, etc., for the ramp step function, when $t_r/\tau_0 = 1.5, 2.5, 3.5$, etc., for the versed-sine step function, and when $t_r/\tau_0 = 2, 3, 4$, etc., for the cycloidal step function. The lowest value of shock transmission is provided by the ramp step function for low values of the time ratio t_r/τ_0.

Effect of Damping. Dimensionless time-histories of the shock transfer response $T_s(\omega_0 t)$ and the shock amplification response $H_s(\omega_0 t)$ for sustained acceleration of the foundation may be defined as follows

$$T_s(\omega_0 t) = A(\omega_0 t)/A_s = \ddot{x}(\omega_0 t)/\ddot{a}_s \qquad (38)$$

$$H_s(\omega_0 t) = \delta(\omega_0 t)\omega_0^2/A_s g = \delta(\omega_0 t)\omega_0^2/\ddot{a}_s \qquad (39)$$

Table 2 — Approximate shock transmissibility and shock amplification factor equations for acceleration shock pulse excitation of the foundation.

Pulse Shape (acceleration)	Velocity Change (V)	Shock Response (T_s or H_s)	Region of Validity
Half-Sine	$(2g/\pi) A_0 t_0$	$4(t_0/\tau_0)$	$t_0/\tau_0 < 0.33$
Rectangular	$g A_0 t_0$	$2\pi(t_0/\tau_0)$	$t_0/\tau_0 < 0.25$
Triangular	$(g/2) A_0 t_0$	$\pi(t_0/\tau_0)$	$t_0/\tau_0 < 0.33$
Versed-Sine	$(g/2) A_0 t_0$	$\pi(t_0/\tau_0)$	$t_0/\tau_0 < 0.33$

where Eqs. (27) and (28) can be employed to define similar expressions for sustained velocity and displacement of the foundation or for a sustained force applied to the isolated mass. Graphical presentations of these shock response time-histories for an isolation system with directly coupled viscous damping subjected to an instantaneous step sustained loading are shown in Figure 23. Isolation system damping is observed to decrease the response maxima of the isolation system below the values that exist for zero damping, and provide a faster decay of the transient vibration response. The undamped shock response is represented by a versed-sine time-history whereas, for values of damping in the range $0 < \zeta < 1$, the shock response decays exponentially to its steady-state value after reaching its maximum magnitude.

The shock transmissibility T_s and the shock amplification factor H_s for an instantaneous step sustained loading, as defined by Eqs. (27) and (28), are presented in Figure 24 for directly coupled viscous damping. For $\zeta < 0.2$, T_s and H_s are very nearly equal. In general, however, the shock transmissibility is greater than the shock amplification factor for a given amount of damping, thereby indicating that directly coupled viscous damping is more effective in reducing the maximum dynamic displacement than in reducing the maximum transmitted acceleration or force.

Isolator Nonlinear Stiffness Characteristics

Various types of isolator nonlinear stiffness characteristics may be employed to achieve a compromise between the transmitted acceleration or force and the resulting displacement that is more acceptable than the combination provided by a linear isolator. Typical stiffness characteristics of passive isolators are illustrated in Figure 25 in the form of static force-deflection curves. The stiffness coefficient k for a linear isolator is $k = F/\delta$ whereas, for nonlinear isolators, the stiffness is given by $k = dF/d\delta$, which corresponds to the slope of the force-deflection curve at a specified equilibrium position.

The "ideal" stiffness characteristic for shock is one having a constant force for all deflections greater than zero, the magnitude of which is equal to the allowable value of $m\ddot{x}_{max}$ or $(F_T)_{max}$. This isolator stiffness characteristic provides maximum storage of energy for a given deflection and, therefore, provides shock isolation with minimum isolator displacement. The ideal shock isolator, however, provides no vibration isolation unless the break-loose force is exceeded, and it generally requires an external force to return the system to the static equilibrium position.

The "ideal" stiffness characteristic for vibration is one having a constant force magnitude (e. g., zero value) for all allowable deflections. This is achieved conceptually by employing an isolator mechanism having a zero stiffness or zero rate of change of force with deflection at the static equilibrium posi-
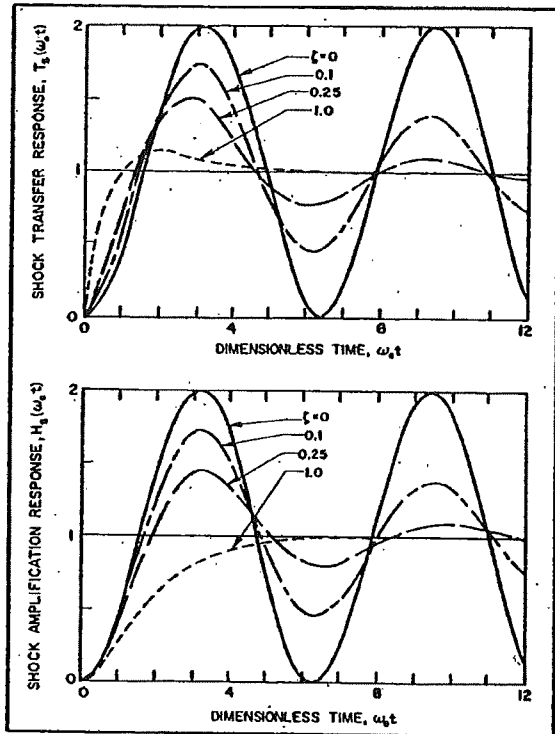

Figure 23 — Shock transfer response and shock amplification response time-histories for an isolation system with directly coupled viscous damping subjected to instantaneous step sustained loading.
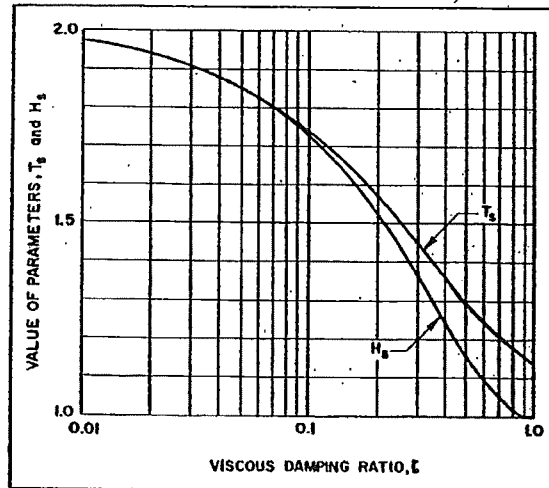

Figure 24 — Shock transmissibility and shock amplification factor for an isolation system with directly coupled viscous damping subjected to instantaneous step sustained loading.

tion. The natural frequency is zero, thereby providing infinite isolation of vibration as long as the displacement is less than the available excursion beyond which the stiffness substantially increases. The ideal vibration isolator, however, provides no shock isolation since it is incapable of storing potential energy. High levels of shock amplification would result because of the high stiffness encountered when the

16

maximum available deflection is reached.

Isolator stiffness characteristics ranging between the "ideal" characteristics for shock and vibration include those identified as *linear, hardening, softening, buckling,* and *bilinear*. The performance of linear isolation systems has been previously discussed. If relative displacement is the most important response parameter, isolators with hardening stiffness characteristics may be employed whereas, if acceleration or force is the most important response parameter, isolators with a softening stiffness characteristic may be selected. Considering elastomeric stiffness elements as an example, the stiffness under pure shear tends to be linear for relatively large strains, whereas the stiffness for pure compression and tension exhibits hardening and softening characteristics, respectively. Bilinear stiffness isolators may be hardening or softening, depending upon the relative values of the two linear stiffnesses that characterize the isolator. A hardening bilinear stiffness characteristic is useful for determining the effects of isolator snubbing or abrupt bottoming and is frequently employed to provide a low initial stiffness for vibration isolation and a relatively high final stiffness to limit the dynamic deflections under shock excitation.[29] An elastic-plastic bilinear stiffness characteristic in the form of an initial linear stiffness followed by a zero stiffness may be used to study a "yielding" isolator that has been deflected into its plastic region. Finally, a buckling stiffness characteristic may be used to derive the benefits of both a hardening and a softening stiffness characteristic at appropriate positions in the isolator deflection range. This type of stiffness characteristic is exhibited by certain cushioning materials, such as elastimeric foam,[30, 31] and by specially designed elastomeric isolators.[29, 32]

A comparison of dynamic response time-histories for an undamped shock isolation system is presented in Figure 26 for hardening, linear, and softening isolator stiffness characteristics, where the acceleration $\ddot{x}(t)$, velocity $\dot{x}(t)$ and relative displacement $\delta(t)$ are shown for velocity shock excitation of the foundation with the system initially at rest. It is assumed that the isolator force is an odd function of isolator deflection; that is, $F(\delta) = -F(-\delta)$ with the origin at the static equilibrium position.

The acceleration and relative displacement time-histories for a linear stiffness isolator are sinusoidal, with maximum magnitudes given by Eqs. (30) and (31), respectively; the isolated mass acquires a velocity equal in value to the velocity change V after a period of time equal to π/ω_0, when the magnitudes of acceleration and relative displacement response are zero. For the hardening stiffness characteristic, a greater magnitude of acceleration is transmitted with less relative displacement than that for the linear system; the isolated mass acquires a velocity equal in value to the velocity change in a shorter period of time; and, the response curves exhibit a "spike" and indicate a shorter natural period of
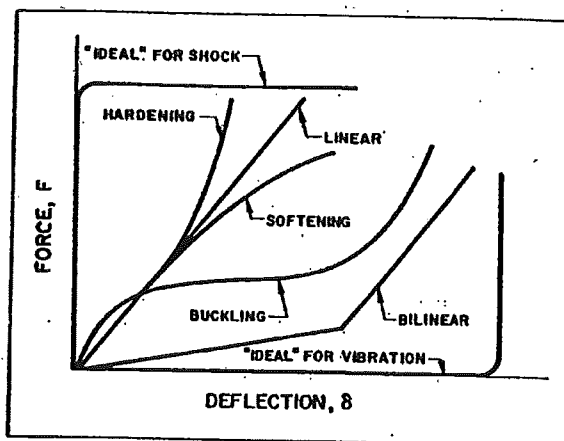

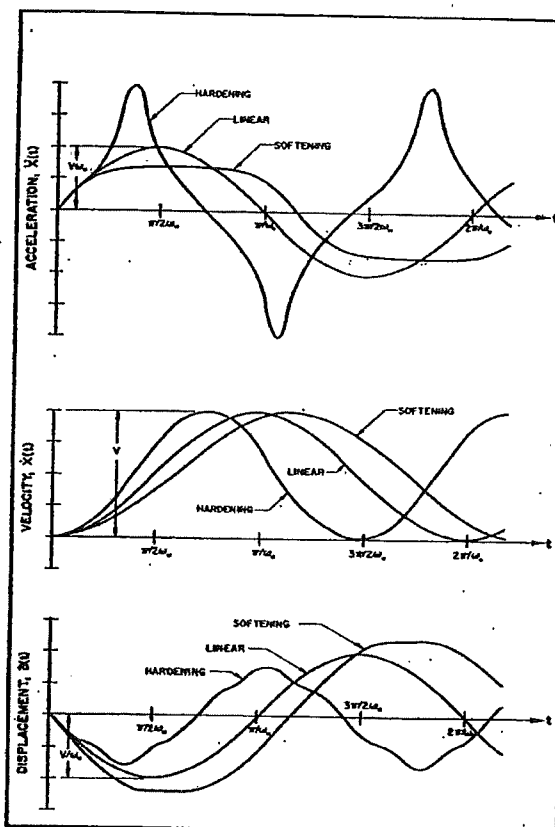Figure 25 — Force-deflection curves indicating various isolator nonlinear stiffness characteristics.

Figure 26 — Response time-histories for velocity shock excitation of undamped isolation systems with hardening, linear, and softening isolator stiffness characteristics.

vibration. For the softening stiffness characteristic, a lower magnitude of acceleration is transmitted with a relative displacement greater than that for a linear system; the isolated mass is slower to acquire a velocity equal in value to the velocity change, and the "flattened" response curves indicate an increased natural period of vibration.

The use of nonlinear stiffness characteristics provides considerable flexibility in tailoring isolator

designs for specific engineering applications. Basic techniques for analyzing and designing nonlinear shock isolators are available in the technical literature,[4, 11, 13, 29-35] including the effects of isolator damping.[33, 36-39] More advanced analysis and automated design procedures have been developed with regard to the problem of mitigating the effects of air, ground and underwater blast shock.[40-42]

Velocity Shock Isolation With Zero Damping. A relatively simple method exists for determining the response of an undamped isolation system with isolators having nonlinear stiffness characteristics subjected to velocity shock excitation. The area under the isolator force-deflection curve represents the potential energy stored by the isolator. Since there is no energy dissipation through damping, the maximum potential energy stored by the isolator for displacements beyond the static equilibrium position equals the maximum kinetic energy associated with the velocity shock condition, as follows

$$mV^2/2 = \int_0^\delta F(\delta)d\delta \qquad (40)$$

where the isolator nonlinear force $F(\delta)$ is related to the response acceleration or force transmitted to the foundation, as follows:

$$F(\delta) = m\ddot{x} = mgA = F_T \qquad (41)$$

Selection of an idealized mathematical force-deflection relation to represent the nonlinear stiffness characteristic of a shock isolator is based either on an analysis of the isolator stiffness mechanism or on experimental force-deflection data. Solution of Eqs. (40) and (41) for a specified isolator force-deflection relation results in the determination of response maxima in terms of the velocity change V and parameters that define the nonlinear characteristics of the isolator stiffness.

Using this analytical approach, design data for undamped isolation systems are determined in terms of dimensionless excitation and response parameters for a variety of isolator stiffness nonlinearities. Shock excitation is expressed in terms of the ratio of velocity change V to a suitable reference velocity. Shock response is expressed in terms of the ratio of acceleration or force and displacement response maxima to suitable reference values that are related either to the response characteristics for a linear isolator or to parameters characteristic of the nonlinear isolator stiffness; the first type of response parameter is useful for comparing the nonlinear isolation system response with that of a reference linear system, whereas the second type is particularly useful for design purposes. Optimum design parameters for the nonlinear isolators are given, corresponding to the condition wherein the transmitted acceleration or force is a minimum. The optimum designs do not necessarily represent the best overall design, however, since an evaluation of the variation of isolation
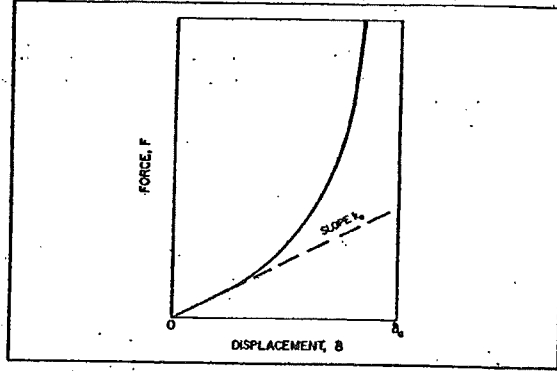

Figure 27 — Force-deflection curve for tangent elasticity isolator.
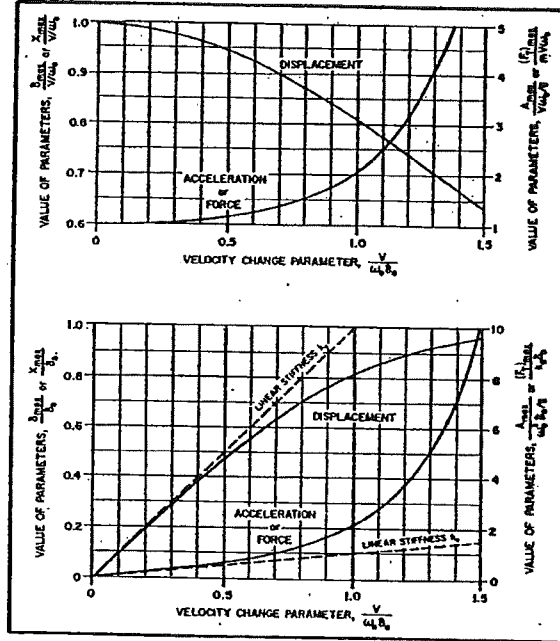

Figure 28 — Acceleration or force and displacement response maxima for velocity shock excitation of an undamped isolation system with tangent elasticity isolators.

system response maxima about the optimum condition may indicate that, for a given application, a combination of acceleration or force and displacement response magnitudes other than the minimax values provided by the optimum design is more desirable. Furthermore, other design considerations such as vibration isolation and sustained loading requirements may necessitate the use of isolator stiffness characteristics that are not compatible with optimum nonlinear stiffness design parameters for velocity shock excitation.

Tangent Elasticity Isolator. A hardening isolator stiffness characteristic may be described in terms of tangent elasticity, which is expressed mathematically by the following force-deflection relation[4, 11, 13, 30]

$$F(\delta) = \frac{2k_0\delta_0}{\pi}\tan\left(\frac{\pi\delta}{2\delta_0}\right) \qquad (42)$$

18

where k_0 is the initial stiffness of the isolator and δ_0 represents the maximum available displacement, as indicated in Figure 27. This force-deflection characteristic may be used to represent an isolator stiffness that increases with displacement and eventually experiences relatively smooth bottoming at a specified maximum displacement.

The acceleration or force and displacement response maxima of an isolation system employing a tangent elasticity isolator for velocity shock excitation are presented in Figure 28. The dimensionless response parameters provided by the upper graph are the ratio of maximum response magnitudes to the magnitudes that would exist for a linear isolator having a stiffness k_0. The lower graph provides the ratio of maximum response magnitudes to parameters that are characteristic of the tangent elasticity force-deflection curve. When compared to the performance of a linear isolator of stiffness k_0, the tangent elasticity isolator provides a lower displacement response and an increased acceleration or force response. For low values of the velocity change V, the performance of the tangent elasticity isolator nearly equals that of the linear isolator, with a deviation in performance apparent for values of velocity change $V > 0.5\ \omega_0\delta_0$, where $\omega_0 = (k_0/m)^{1/2}$.

The *optimum design* for tangent elasticity isolators corresponds to the condition wherein the acceleration or force response magnitude is a minimum for a specified maximum available displacement δ_0. The optimum values of the initial stiffness k_0 and the natural frequency ω_0 are as follows

$$(k_0)_{op} = 1.55mV^2/\delta_0{}^2 \qquad (43)$$

$$(\omega_0)_{op} = 1.24V/\delta_0 \qquad (44)$$

The resulting optimum values of acceleration or force and displacement response magnitudes are

$$(A_{max})_{op} \text{ or } \left[\frac{(F_T)_{max}}{mg}\right]_{op} = 1.95V^2/g\delta_0 \qquad (45)$$

$$(\delta_{max})_{op} \text{ or } (X_{max})_{op} = 0.7\delta_0 \qquad (46)$$

The optimum design condition, which corresponds to a value of the velocity change parameter $V/\omega_0\delta_0 = 0.8$, results in an acceleration or force response magnitude that is 56 percent greater than the corresponding response magnitude for a linear isolator of stiffness k_0, while the displacement response magnitude is 13 percent less than that of the linear isolator.

Hyperbolic Tangent Elasticity Isolator. A softening isolator stiffness characteristic may be described in terms of *hyperbolic tangent elasticity*, which is expressed by the following force-deflection relation[11, 13]

$$F(\delta) = F_0 \tanh\left(\frac{k_0\,\delta}{F_0}\right) \qquad (47)$$

where k_0 is the initial stiffness of the isolator and F_0 represents the maximum allowable force, as indi-
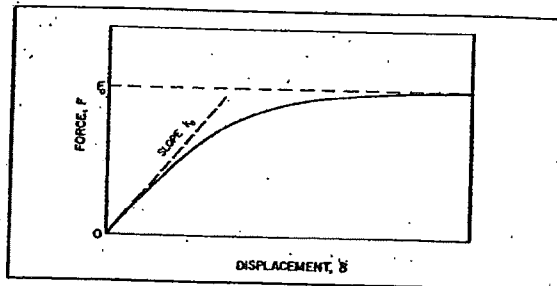

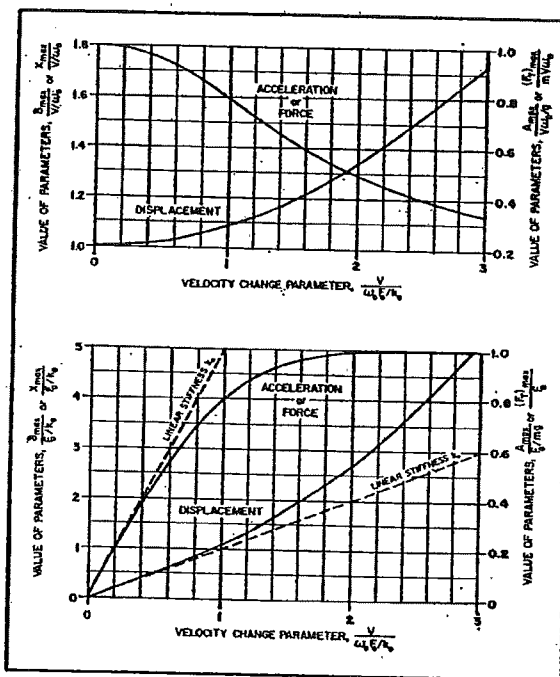*Figure 29 — Force-deflection curve for hyperbolic tangent elasticity isolator.*

Figure 30 — Acceleration or force and displacement response maxima for velocity shock excitation of an undamped isolation system with hyperbolic tangent elasticity isolators.

cated in Figure 29. This type of stiffness characteristic may be used to represent an isolator that exhibits a stiffness that decreases with displacement and eventually approaches zero.

The acceleration or force and displacement response maxima of an isolation system employing a hyperbolic tangent elasticity isolator for velocity shock excitation are presented in Figure 30. The dimensionless response parameters provided by the upper graph are the ratio of maximum response magnitudes to the magnitudes that would exist for a linear isolator having a stiffness k_0. The lower graph provides the ratio of maximum response magnitudes to parameters that are characteristic of the hyperbolic tangent elasticity force-deflection curve. When compared to the performance of a linear isolator of stiffness k_0, the hyperbolic tangent elasticity isolator provides a lower acceleration or force response and an increased displacement response. For

SOUND AND VIBRATION •

19

low values of the velocity change V, the performance of the hyperbolic tangent elasticity isolator nearly equals that of the linear isolator, with a deviation in performance apparent for values of velocity change $V > 0.5\ \omega_0 F_0/k_0$, where $\omega_0 = (k_0/m)^{1/2}$.

The *optimum design* hyperbolic tangent elasticity isolator corresponds to the "ideal" shock isolator stiffness for which $k_0 = \infty$ and a constant force F_0 is provided for all deflections as illustrated in Figure 25. The minimax displacement response for a specified maximum magnitude of acceleration or force is given by

$$(\delta_{max})_{op} \text{ or } (X_{max})_{op} = mV^2/2F_0 \qquad (48)$$

and the acceleration or force response magnitude is as follows

$$(A_{max})_{op} \text{ or } \left[\frac{(F_T)_{max}}{mg}\right]_{op} = F_0/mg \qquad (49)$$

For a specified acceleration or force response magnitude, the optimum design condition results in a displacement response magnitude equal to one-half that of a linear isolator.

Bilinear Stiffness Isolators. A hardening or softening stiffness characteristic may be represented by a *bilinear stiffness* isolator, which exhibits different l near stiffnesses over two isolator deflection ranges. The force-deflection relations are given by[11]

$$F(\delta) = k_0\delta \qquad (0 < \delta < \delta_0)$$

$$(50)$$

$$F(\delta) = k_1\delta - (k_1 - k_0)\delta_0 \qquad (\delta_0 < \delta < \infty)$$

where k_0 is the initial stiffness of the isolator, k_1 is the stiffness of the isolator for large deflections, and δ_0 is the deflection at which the isolator stiffness changes from k_0 to k_1, as indicated in Figure 31. A hardening stiffness characteristic is exhibited when $k_1 > k_0$, and the effect of *isolator snubbing* or *bottoming* may be evaluated by considering appropriately large values of the ratio k_1/k_0. By selecting $k_1 < k_0$, a softening stiffness characteristic is obtained, and setting $k_1 = 0$ provides the force-deflection characteristic of an *elastic-plastic* (yielding) isolator.

Hardening Bilinear Stiffness Isolator:

The acceleration or force and displacement response maxima of an isolation system employing a *hardening bilinear stiffness isolator* for velocity shock excitation are presented in Figure 32. Curves above the $k_1/k_0 = 1.0$ curve provide the maximum acceleration or force response, whereas those below provide the maximum displacement response. The dimensionless response parameters provided by the upper graph are the ratio of maximum response magnitudes to the magnitudes that would exist for a linear isolator having a stiffness k_0. The lower graph provides the ratio of maximum response magnitudes to parameters that are characteristic of the bilinear force-deflection curve. When compared to the performance of a linear isolator of stiffness k_0,
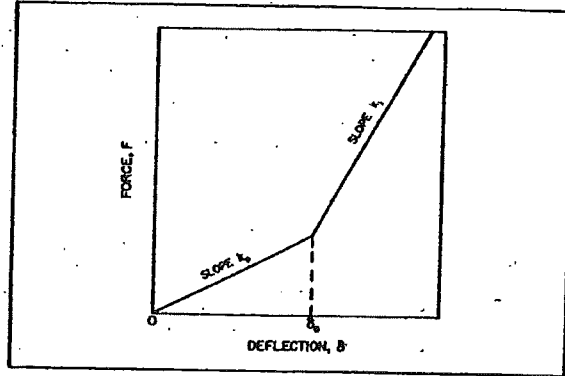

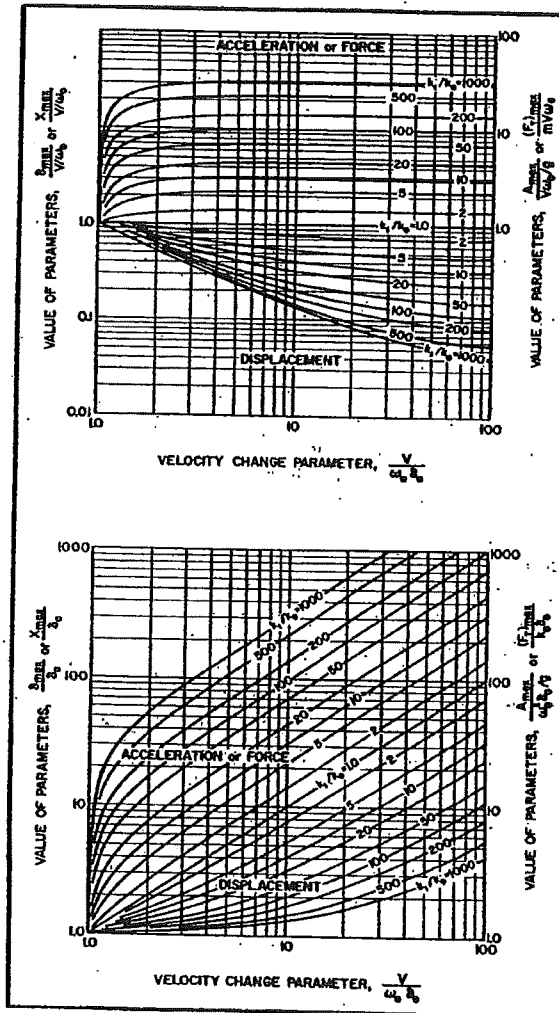Figure 31 — Force-deflection curve for bilinear stiffness isolator.

Figure 32.— Acceleration or force and displacement response maxima for velocity shock excitation of an undamped isolation system with hardening bilinear stiffness isolators.

the hardening bilinear stiffness isolator provides a lower displacement response and an increased acceleration or force response. For large values of the velocity change parameter $V/\omega_0\delta_0$, the acceleration

20

or force response magnitude approaches $(k_1/k_0)^{1/2}$ times that for a linear isolator of stiffness k_0, while the displacement response magnitude approaches $(k_0/k_1)^{1/2}$ times the linear isolator displacement. For values of velocity change $V \leq \omega_0 \delta_0$ where $\omega_0 = (k_0/m)^{1/2}$, the isolation system responds as a linear system, since the deflection is in the range $0 < \delta < \delta_0$.

For $V \geq \omega_0 \delta_0$, the *optimum design* for a hardening bilinear stiffness isolator corresponds to the condition wherein the acceleration or force response maxima are a minimum for specified values of stiffness k_1 and the deflection δ_0. The optimum values of the initial stiffness k_0 and the natural frequency ω_0 are as follows

$$(k_0)_{op} = k_1/2 \tag{51}$$

$$(\omega_0)_{op} = \sqrt{k_1/2m} \tag{52}$$

The acceleration or force and displacement response magnitudes for the optimum design condition of $k_1/k_0 = 2$ are

$$(A_{max})_{op} = \left[\frac{F_{T\,max}}{mg}\right]_{op} = \frac{k_1 \delta_0}{2mg} \sqrt{\frac{4mV^2}{k_1 \delta_0^2} - 1} \tag{53}$$

$$(\delta_{max})_{op} = \frac{\delta_0}{2}\left[1 + \sqrt{\frac{4mV^2}{k_1 \delta_0^2} - 1}\right] \tag{54}$$

For values of the velocity change $V > 20\,\omega_0\delta_0$, the optimum acceleration or force response magnitude is 41 percent greater than the corresponding response magnitude for a linear isolator of stiffness k_0, while the optimum displacement response magnitude is 29 percent less than that of the linear isolator.

Elastic-Plastic Isolator:

The maximum displacement response of an isolation system employing an *elastic-plastic isolator* for velocity shock excitation is presented in Figure 33. The upper and lower curves provide the ratio of maximum response displacement to the displacement δ_0 and to the displacement V/ω_0 that would exist for a linear isolator having a stiffness k_0, respectively. The acceleration or force response magnitude is given by

$$A_{max} = \frac{(F_T)_{max}}{mg} = V\omega_0/g \qquad (V \leq \omega_0\delta_0) \tag{55}$$

$$A_{max} = \frac{(F_T)_{max}}{mg} = k_0\,\delta_0/mg \qquad (V \geq \omega_0\delta_0) \tag{56}$$

where $\omega_0 = (k_0/m)^{1/2}$.

The *optimum design* elastic-plastic isolator corresponds to the "ideal" shock isolator stiffness for which $k_0 = \infty$ and a constant force F_0 is provided for all deflections. The displacement and acceleration or force response magnitudes are given by Eqs. (48) and (49), respectively.
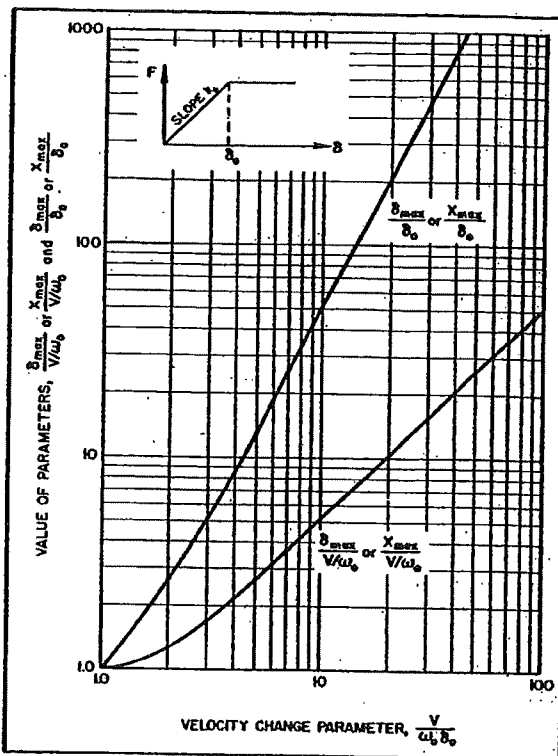

Figure 33 — Displacement response maxima for velocity shock excitation of an undamped isolation system with elastic-plastic (yielding) isolators.
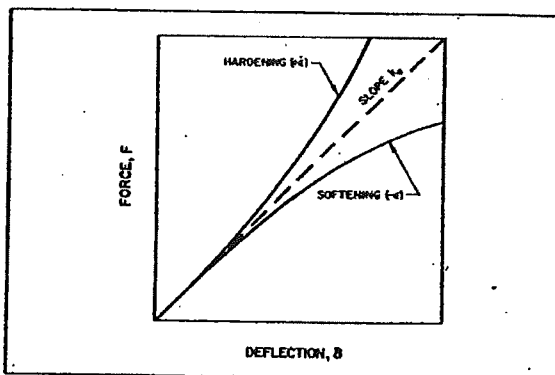

Figure 34 — Force-deflection curves for polynomial elasticity isolators.

Polynomial Elasticity Isolators. A continuously varying hardening or softening isolator stiffness characteristic may be described in terms of *polynomial elasticity*, which is expressed mathematically by the followng force-deflection relation

$$F(\delta) = k_0 \delta \pm \epsilon_n \delta^n \qquad (\delta > 0) \tag{57}$$

where k_0 is the initial stiffness of the isolator, and the coefficient ϵ_n and the exponent n are positive numbers. To account for both positive and negative values of deflection, the force-deflection relation is written in the following form:

$$F(\delta) = -F(-\delta) = k_0 \delta \pm \epsilon_n|\delta^n|sgn(\delta) \tag{58}$$

SOUND AND VIBRATION •

Figure 35 — Acceleration or force and displacement response maxima for velocity shock excitation of an undamped isolation system with hardening quadratic elasticity isolators.
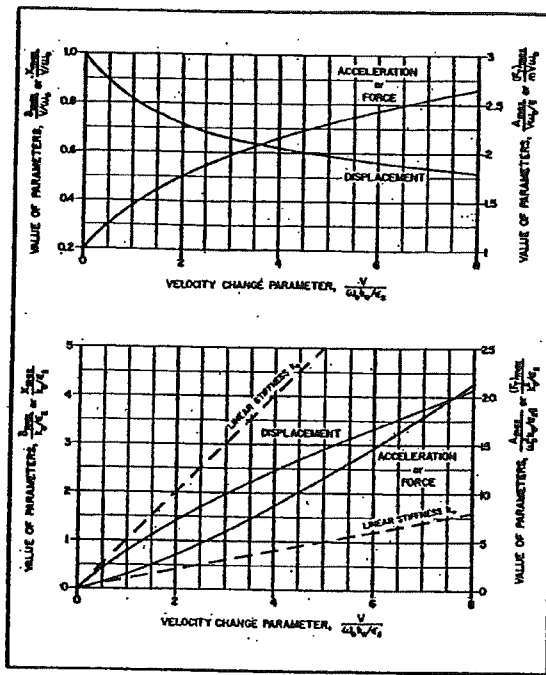

Figure 37 — Acceleration or force and displacement response maxima for velocity shock excitation of an undamped isolation system with hardening cubic elasticity isolators.

Figure 36 — Acceleration or force and displacement response maxima for velocity shock excitation of an undamped isolation system with softening quadratic elasticity isolators.
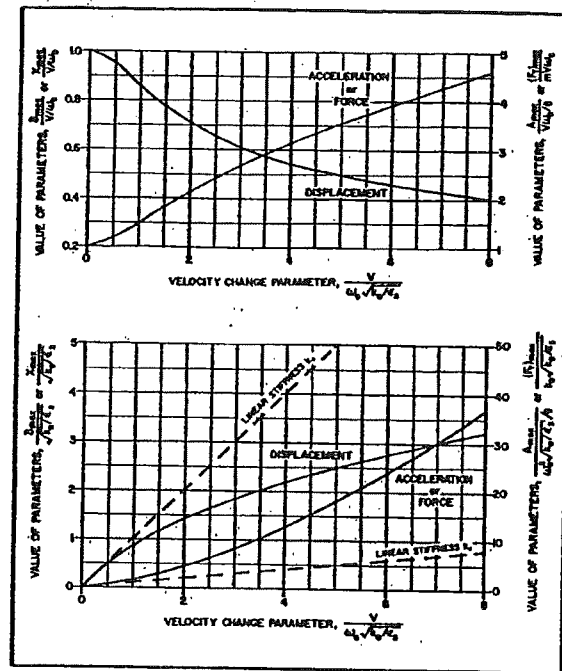

Figure 38 — Acceleration or force and displacement response maxima for velocity shock excitation of an undamped isolation system with softening cubic elasticity isolators.
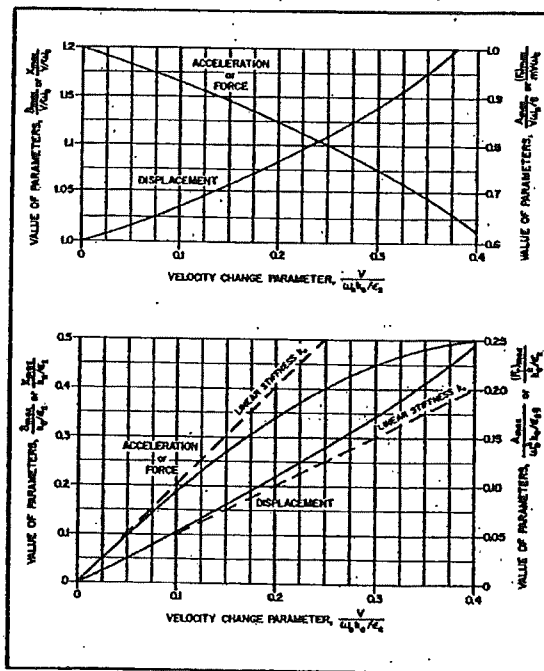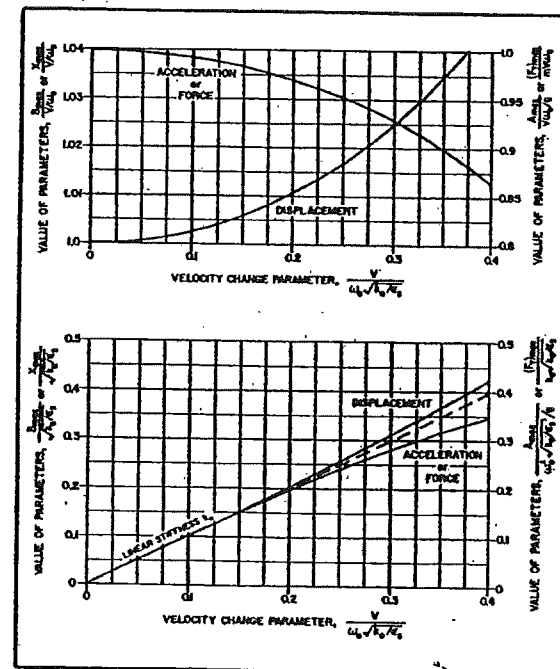
The plus sign in Eqs. (57) and (58) provides a hardening stiffness characteristic and the minus sign provides a softening stiffness characteristic, as illustrated in Figure 34. The higher the values of ϵ_n and

n, the more severe the stiffness nonlinearity.

Setting $n = 2$ and 3 provides equations that represent quadratic elasticity and cubic elasticity, respectively. Hence, an isolator with quadratic elas-

22

ticity is described by the following force-deflection equation

$$F(\delta) = k_0 \delta \pm \epsilon_2 \delta^2 \quad (\delta > 0) \quad (59)$$

and, for *cubic elasticity*, the applicable equation is

$$F(\delta) = k_0 \delta \pm \epsilon_3 \delta^3 \quad (\delta > 0) \quad (60)$$

Care must be exercised in employing polynomial expressions to represent softening stiffness characteristics. As the deflection increases, the stiffness of a softening polynomial elasticity isolator decreases and becomes negative for sufficiently high values of deflection. Negative stiffnesses are avoided if the isolator deflection is limited as follows

$$\delta_{max} \leq \left(\frac{k_0}{n\epsilon_n}\right)^{1/(n-1)} \quad (61)$$

The acceleration or force response maxima that occurs at the maximum allowable isolator deflection, as defined by the equality of Eq. (61), is given by

$$A_{max} \text{ or } \frac{(F_T)_{max}}{mg} = \frac{k_0}{mg}\left(\frac{n-1}{n}\right)\left(\frac{k_0}{n\epsilon_n}\right)^{1/(n-1)} \quad (62)$$

For softening quadratic elasticity, $\delta_{max} \leq k_0/2\epsilon_2$ and $(F_T)_{max} = k_0^2/4\epsilon_2$ whereas, for softening cubic elasticity, $\delta_{max} \leq (k_0/3\epsilon_3)^{1/2}$ and $(F_T)_{max} = (2k_0/3)(k_0/3\epsilon_3)^{1/2}$. To ensure that the isolator exhibits a positive stiffness, the maximum permissible values of velocity change are approximately $V_{max} = 0.4 \ \omega_0 k_0/\epsilon_2$ and $V_{max} = 0.5 \ \omega_0 (k_0/\epsilon_3)^{1/2}$ for quadratic and cubic elasticity, respectively.

The acceleration or force and displacement response maxima of isolation systems employing hardening and softening quadratic elasticity isolators for velocity shock excitation are presented in Figures 35 and 36, respectively. The corresponding isolation system response maxima for hardening and softening cubic elasticity are presented in Figures 37 and 38, respectively. The dimensionless response parameters provided by the upper graphs are the ratio of maximum response magnitudes to the magnitudes that would exist for a linear isolator having a stiffness k_0. The lower graphs provide the ratio of maximum response magnitudes to parameters that are characteristic of the quadratic elasticity or cubic elasticity force-deflection curves.

References

1. J. E. Ruzicka, Characteristics of Mechanical Vibration and Shock, *Sound and Vibration*, 1 (April 1967, pp. 14-31).
2. J. E. Ruzicka, Active Vibration and Shock Isolation, Paper No. 680747, *SAE Trans.*, 77 (1969, pp. 2872-2886).
3. J. T. Brock and H. P. Olesen, The Frequency Analysis of Mechanical Shock, *Sound and Vibration*, 4 (March 1970, pp. 30-37).
4. C. E. Crede, *Vibration and Shock Isolation*, John Wiley and Sons, New York (1951, p. 93).
5. C. E. Crede, "Vibration and Shock Isolators, *Machine Design* (Aug. 1954).
6. R. D. Cavanaugh, Air Suspension and Servo-Controlled Isolation Systems, *Shock and Vibration Handbook* (edited by C. M. Harris, and C. E. Crede), Vol. 2, Chap. 33, McGraw-Hill Book Co., New York (1961).
7. J. E. Ruzicka, Vibration Control, *Electro-Technology*, 72 (Aug. 1963, pp. 64-82).
8. S. Kunica, Servo-Controlled Pneumatic Isolators — Their Properties and Applications, ASME Paper No. 65-WA/MD-12 (Nov. 1965).
9. J. E. Ruzicka, Resonance Characteristics of Unidirectional Viscous and Coulomb-Damped Vibration Isolation Systems, *Trans. ASME, Jour. of Eng. for Industry*, 89, Series B, No. 4 (Nov. 1967, pp. 729-740).
10. S. Rubin, Concepts in Shock Data Analysis, *Shock and Vibration Handbook* (edited by C. M. Harris, and C. E. Crede), Vol. 2, Chap. 23, McGraw-Hill Book Co., New York (1961).
11. R. D. Mindlin, Dynamics of Package Cushioning, *Bell System Technical Journal*, 24 (July-Oct. 1945, pp. 353-461). (Also published as Bell Telephone System Technical Publications Monograph B-1369).
12. R. D. Mindlin, F. W. Stubner, and H. L. Cooper, Response of Damped Elastic Systems to Transient Disturbances, *SESA Proceedings*, V, 2 (1948, pp. 69-76).
13. R. E. Newton, Theory of Shock Isolation, *Shock and Vibration Handbook* (edited by C. M. Harris, and C. E. Crede), Vol. 2, Chap. 31 McGraw-Hill Book Co., New York (1961).
14. E. C. Fischer, Theory of Equipment Design, *Shock and Vibration Handbook* (edited by C. M. Harris, and C. E. Crede), Vol. 3, Chap. 42, McGraw-Hill Book Co., New York (1961).
15. R. S. Ayre, Transient Response to Step and Pulse Functions, *Shock and Vibration Handbook* (edited by C. M. Harris, and C. E. Crede), Vol. 1, Chap. 8, McGraw-Hill Book Co., New York (1961).
16. E. H. Schell, Spectral Characteristics of Some Practical Variations in the Half-Sine and Saw-Tooth Pulses, Air Force Report AFFDL-TR-64-175 (DDC Report AD 613 024) (Jan. 1965). (Also available in *Shock and Vibration Bulletin*, No. 34, Part 3, Dec. 1964, pp. 223-251).
17. J. J. Marous and E. H. Schell, An Analog Computer Technique for Obtaining Shock Spectra, *Shock and Vibration Bulletin*, No. 33, Part II (Feb. 1964, pp. 182-194).
18. R. R. Luke, The Impact Response of a Single Degree of Freedom System with Viscous Damping, University of Texas Structural Mechanics Research Laboratory, DDC Report AD 246 942 (June 1960).
19. T. F. Derby and P. C. Calcaterra, Response and Optimization of an Isolation System with Relaxation Type Damping, NASA CR-1542 (May 1970). (A shortened version of this report appears under the same title in *Shock and Vibration Bulletin*, No. 40, Part 5, Dec. 1969, pp. 203-216).
20. J. C. Snowdon, Steady-State and Transient Behavior of Two- and Three-Element Isolation Mountings, *Jour. Acous. Soc. of Amer.*, 35, 3 (March 1963, pp. 397-403).
21. K. Klotter, Free Oscillations of Systems Having Quadratic Damping and Arbitrary Restoring Forces, *Trans. ASME, Jour. Appl. Mech.*, 22, 4 (1955, pp. 493-499).
22. L. S. Jacobsen and R. S. Ayre, *Engineering Vibrations*, McGraw-Hill Book Co., New York (1958).
23. R. O. Brooks, The Use of Graphical Techniques to Analyze Shock Motions of Lightly Damped Linear Spring Mass Systems, *Shock and Vibration Bulletin*, No. 33, Part II, pp. 195-210.

24. Anon., A guide for the Design of Shock Isolation Systems for Underground Protective Structures, Air Force Report AFSWC-TDR-62-64 (DDC Report AD 298 578), Dec. 1962.

25. J. E. Ruzicka and R. D. Cavanaugh, New Method for Vibration Isolation, *Machine Design*, 30, 21 (Oct. 16, 1958, pp. 114-121).

26. L. S. Jacobsen and R. S. Ayre, A Comprehensive Study of Pulse and Step-Type Loads on a Simple Vibratory Structure, Stanford University Vibration Research Laboratory, Technical Report No. 16 (Jan. 1952).

27. M. V. Barton, V. Chobotov, and Y. C. Fung, A Collection of Information on Shock Spectrum of a Linear System, DDC Report AD 607 815 (July 1961).

28. I. Vigness, Elementary Considerations of Shock Spectra, *Shock and Vibration Bulletin*, No. 34, Part 3 (Dec. 1964, pp. 211-222).

29. C. M. Salerno, 2K Approach for Vibration and Shock Protection for Shipboard Equipments, *Shock and Vibration Bulletin*, No. 40, Part 7 (Dec. 1969, pp. 233-241).

30. P. E. Franklin and M. T. Hatae, Packaging Design, *Shock and Vibration Handbook* (edited by C. M. Harris and C. E. Crede), Vol. 3, Chap. 41, McGraw-Hill Book Co., New York (1961).

31. G. S. Mustin, *Theory and Practice of Cushion Design*, Monograph No. SVM-2, Shock and Vibration Information Center, Washington, D. C. (1968).

32. C. E. Crede and S. E. Young, Theoretical and Experimental Investigation of Buckling Shock Mount, *SESA Proceedings*, 5, 2 (1948, pp. 144-153).

33. W. T. Thompson, Shock Spectra of a Nonlinear System, *Trans. ASME, Jour. Appl. Mech.*, 27, Series E, No. 3 (Sept. 1960, pp. 528-534).

34. Y. C. Fung and M. V. Barton, Shock Response of a Nonlinear System, *Trans. ASME, Jour. of Appl. Mech.*, 29, Series E, No. 3 (Sept. 1962, pp. 465-476).

35. S. T. Ariaratnam, Response of Nonlinear System to Pulse Excitation, *Jour. of Mech. Eng. Science*, 6, 7 (March 1964, pp. 26-31).

36. J. C. Snowdon, Response of Nonlinear Shock Mountings to Transient Foundation Displacements, *Jour. Acous. Soc. of Amer.*, 33, 10 (Oct. 1961, pp. 1295-1304).

37. J. C. Snowdon, Transient Response of Nonlinear Isolation Mountings to Pulselike Displacements, *Jour. Acous. Soc. of Amer.*, 35, 3 (March 1963, pp. 389-396).

38. J. C. Snowdon, *Vibration and Shock in Damped Mechanical Systems*, John Wiley and Sons, Inc., New York (1968).

39. J. D. Kemper and R. S. Ayre, Optimum Damping and Stiffness in Nonlinear Single-Degree-of-Freedom Systems. II. Velocity Shock, *Jour. Acoust. Soc. of Amer.*, 47, 3 (Part 2) (March 1970, pp. 852-856).

40. A. S. Veletsos and N. M. Newmark, Design Procedures for Shock Isolation Systems of Underground Protective Structures (Response Spectra of Single-Degree-of-Freedom Elastic and Inelastic Systems), Air Force Report RTD-TDR-63-3096, Vol. III (DDC Report AD 444 989) (June 1964).

41. Anon., Guide for the Selection and Application of Shock Mounts for Shipboard Equipment, Navy Report NAVSHIPS 0940-000-3010 (Feb. 1967).

42. D. M. Rogers, G. Urmston, and C. Ip, A Method for Designing Linear and Nonlinear Shock Isolation Systems for Underground Missile Facilities, Air Force Report BSD-TR-67-173 (DDC Report AD 818 395) (June 1967).

BARRY CONTROLS